

Supplementary Information for

Aggresomal Sequestration and STUB1-Mediated Ubiquitylation during Mammalian Proteophagy of Inhibited Proteasomes

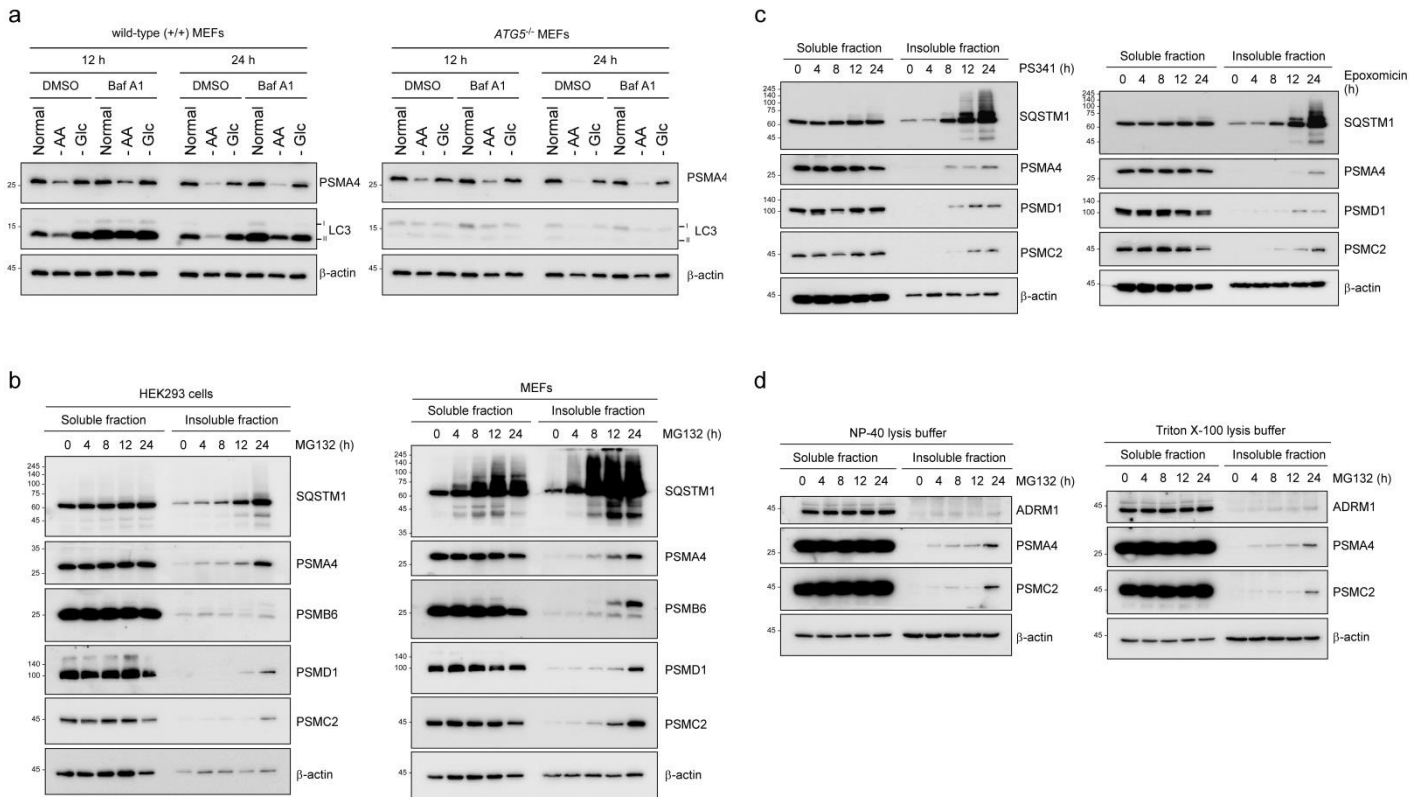
Won Hoon Choi, Yejin Yun, Seoyoung Park, Jun Hyoung Jeon, Jeeyoung Lee, Jung Hoon Lee, Su-A Yang, Nak-Kyoon Kim, Chan Hoon Jung, Yong Tae Kwon, Dohyun Han, Sang Min Lim, and Min Jae Lee*

*Min Jae Lee
Email: minjlee@snu.ac.kr

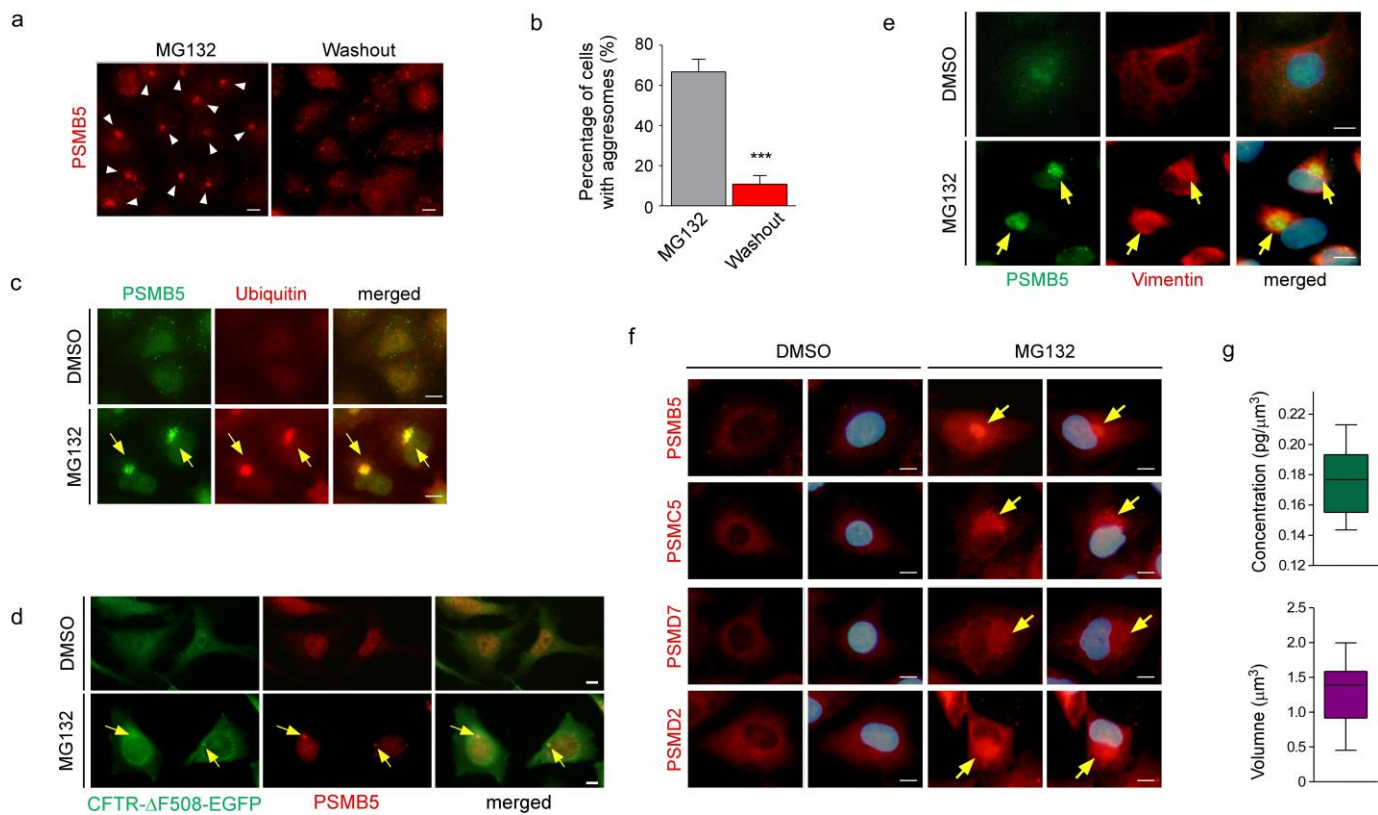
This PDF file includes:

Supplementary Figures 1 to 9
Supplementary Methods
Supplementary References
Supplementary Table 1

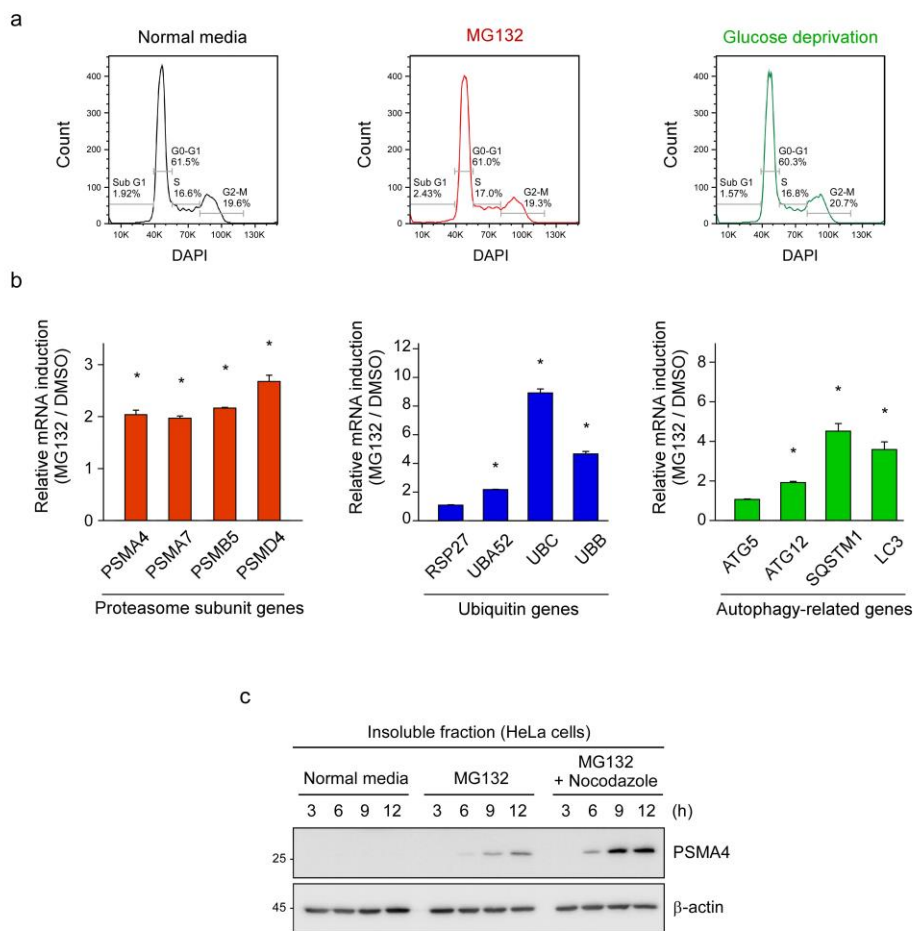
SUPPLEMENTARY FIGURES



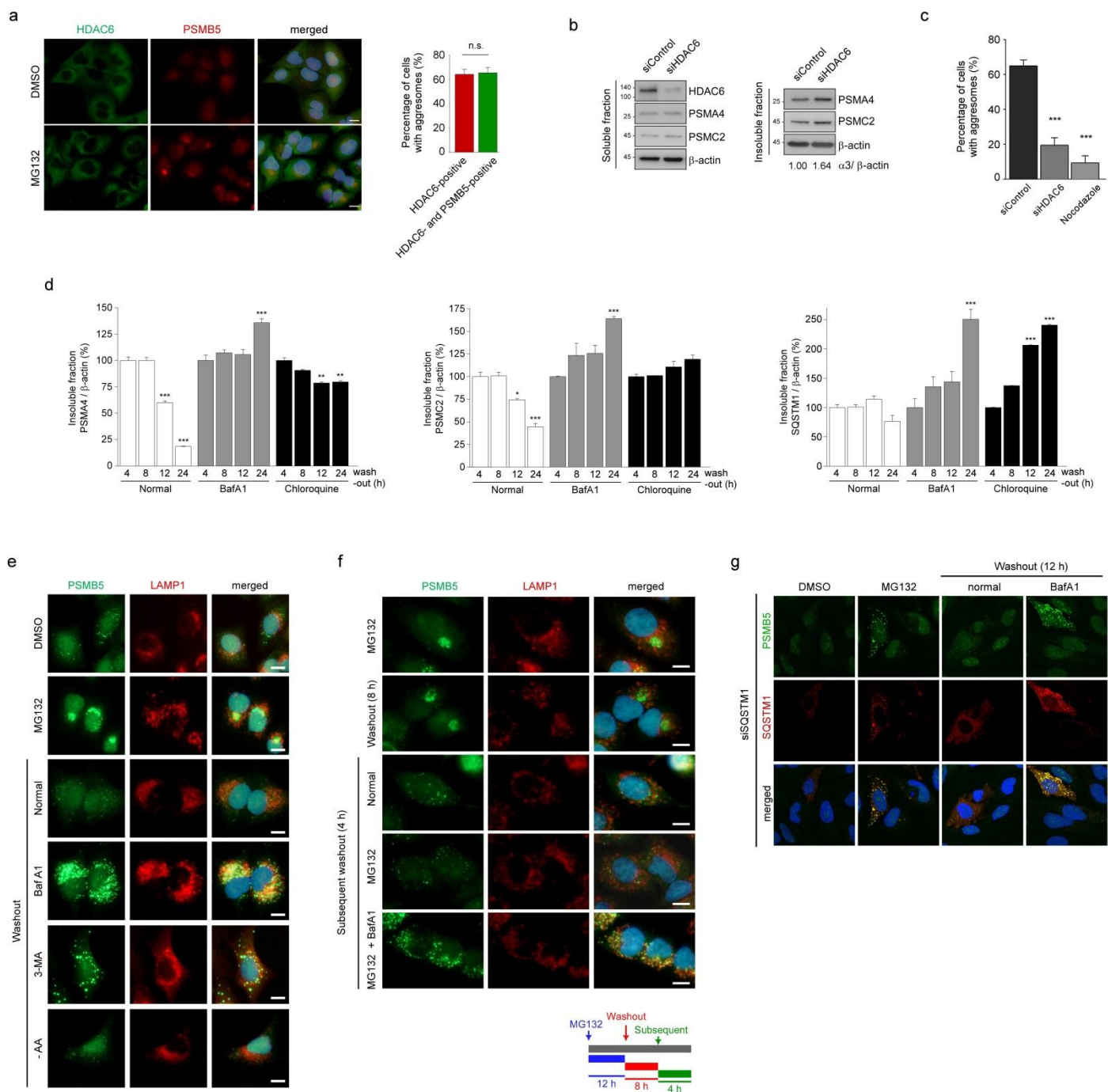
Supplementary Figure 1. Changes of proteasome amounts in the soluble and insoluble fractions. (a) Induction of autophagy had little effect on the proteasome levels in the soluble fraction. Wild-type (+/+) or *ATG5*-null (*ATG5*^{-/-}) mouse embryonic fibroblasts (MEFs) were treated with a nutrient-deprived medium (amino acid-free [- AA] or glucose-free [- Glc]) in the presence or absence of bafilomycin A1 (BafA1; 100 nM) for 12 h or 24 h. Whole-cell extracts (WCEs) were prepared from the Triton-X-100-based lysis buffer, and the samples from the soluble fraction were subjected to SDS-PAGE and immunoblotting (IB) for PSMA4/ α 3, LC3, and β -actin. Of note, the reduced levels of proteasome subunit PSMA4 under the nutrient deprivation conditions was not recovered when autophagy was either genetically or chemically inhibited, indicating that bulk autophagy hardly results in the degradation of proteasome subunits. **(b)** Significantly accumulated proteasome subunits in the Triton-X-100-insoluble fractions were detected in different cell types such as HEK293 cells and mouse embryonic fibroblasts (MEFs) as in A549 cells. **(c)** Both reversible and irreversible proteasome inhibitors, such as PS341 and epoxomicin, respectively, induced the accumulation of proteasomes in the insoluble fraction of WCEs from A549 cells. **(d)** Lysis buffers containing different detergents, such as NP-40 (1%) or Triton X-100 (1%) showed comparable consequences for the proteasome segregation in A549 cells. These data complement Figs. 1a and 1b.



Supplementary Figure 2. Inhibited proteasomes were localized in the juxtannuclear aggresome after prolonged MG132 treatment. (a) Low-magnification images of the juxtannuclear inclusion body formed in A549 cells after 12 h treatment with MG132 (10 μ M) with or without media washout (12 h). Immunofluorescence staining (IFS) for PSMB5 (red). Most cells showed proteasome-positive signals usually as one large punctum near the nucleus. (b) Quantitation of (a). Percentage of cells with aggresomes after MG132 treatment (10 μ M for 12 h) or MG132 treatment followed with media washout (12 h) were counted and plotted as mean \pm SD of three independent experiments with >1,000 cells. ***, $p < 0.001$ (two-tailed Student's t test). (c) Proteasome-positive puncta (PSMB5, green) were found to be colocalized with Ub (red) in MG132-treated A549 cells. (d) Cystic fibrosis transmembrane conductance regulator (CFTR)- Δ F508 (green), which is a misfolded protein generated during the translational process, was found to colocalize with the proteasome-positive cytoplasmic puncta (PSMB5, red). (e) IFS using anti-vimentin antibody. A549 cells were treated with 5 μ M MG132 for 12 h. (f) The RP subunits such as PSMC5, PSMD2, PSMD5 were localized in an enlarged juxtannuclear inclusion body similar to that of the CP subunit PSMB5 after the prolonged MG132 treatment. Scale bars = 10 μ m. These data complement Fig. 1c. (g) Quantitative analysis of tomographic images, measuring the mean volume and concentration of the aggresomes (*see* Methods for details). A box-and-whisker plot with N = 29. These data complement Figs. 1d and 1e.

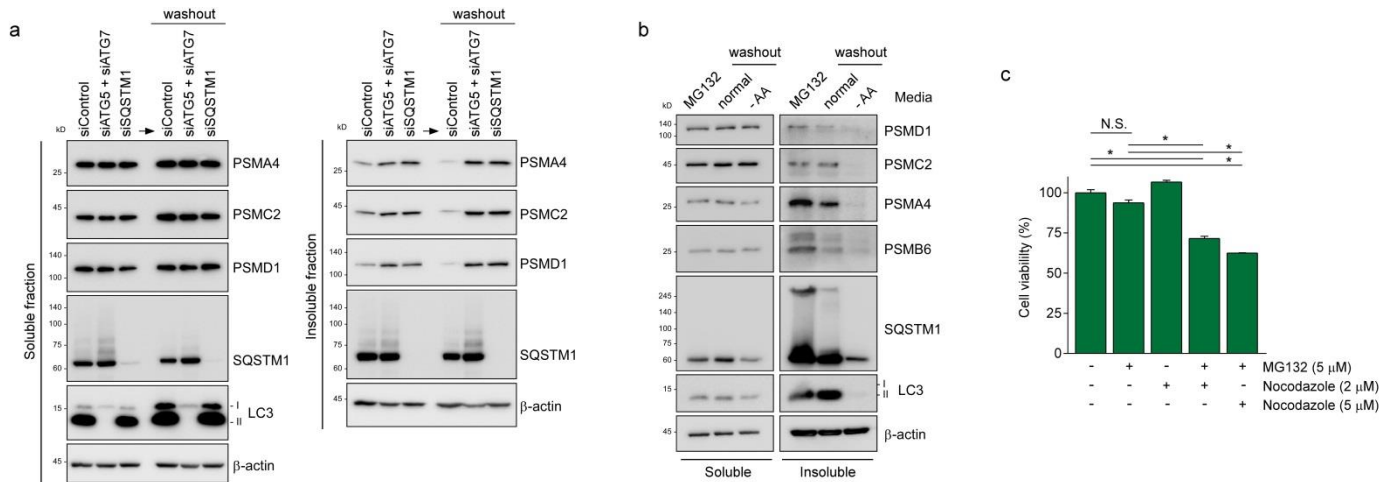


Supplementary Figure 3. Consequences of prolonged treatment with the proteasome inhibitor. (a) Fluorescence-activated cell sorting (FACS) analysis was performed to quantify DNA contents and showed little effect of the proteasome inhibitor MG132 (5 μ M, 6 h) or glucose deprivation (6 h) on the cell cycle. HeLa cells treated with either MG132 or a glucose-free medium were stained with 4',6'-diamidino-2-phenylindole (DAPI) and then analyzed by FACS. (b) Total RNA was isolated from HeLa cells after the treatment with MG132 (5 μ M) for 12 h, and quantitative RT-PCR analyses were performed on proteasome subunit genes, ubiquitin B (*UBB*), ubiquitin C (*UBC*), and autophagy-related genes. The *GAPDH* mRNA levels were used to normalize the other mRNA levels. Statistical significance was analyzed via the means \pm SD from three independent experiments (n = 3). *, $p < 0.01$ (one-way analysis of variance (ANOVA) with Bonferroni's multiple comparison test). (c) Deposition of proteasomes in the insoluble fractions of HeLa cells when treated with MG132 (5 μ M) or with MG132 plus nocodazole (1 μ M) 12 h. These data supplement Fig. 1g.

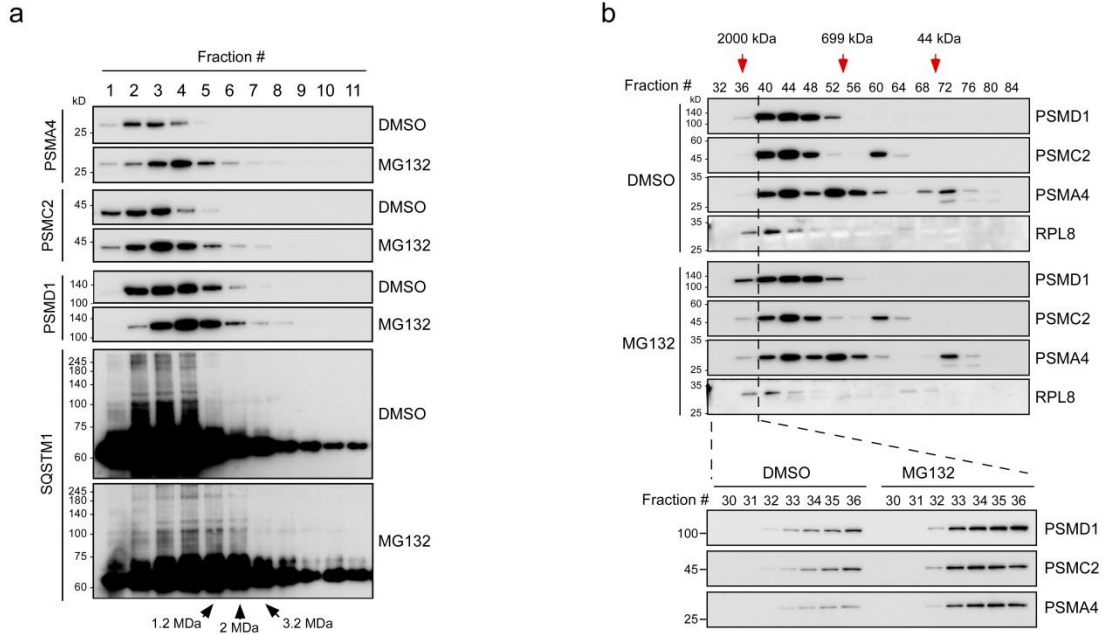


Supplementary Figure 4. Essential roles of HDAC6 and autophagy in the segregation and degradation of inhibited proteasomes, respectively. (a) (*left*) Endogenous HDAC6 in A549 cells was immunostained after treatment with DMSO or 5 μ M MG132 for 12 h, which was found to strongly colocalize with the proteasome-positive inclusion body. IFS with anti-HDAC6 (green) and anti-PSMB5 (red) antibodies. Scale bars = 10 μ m. (*right*) Quantitation of the percentage of cells containing HDAC6-

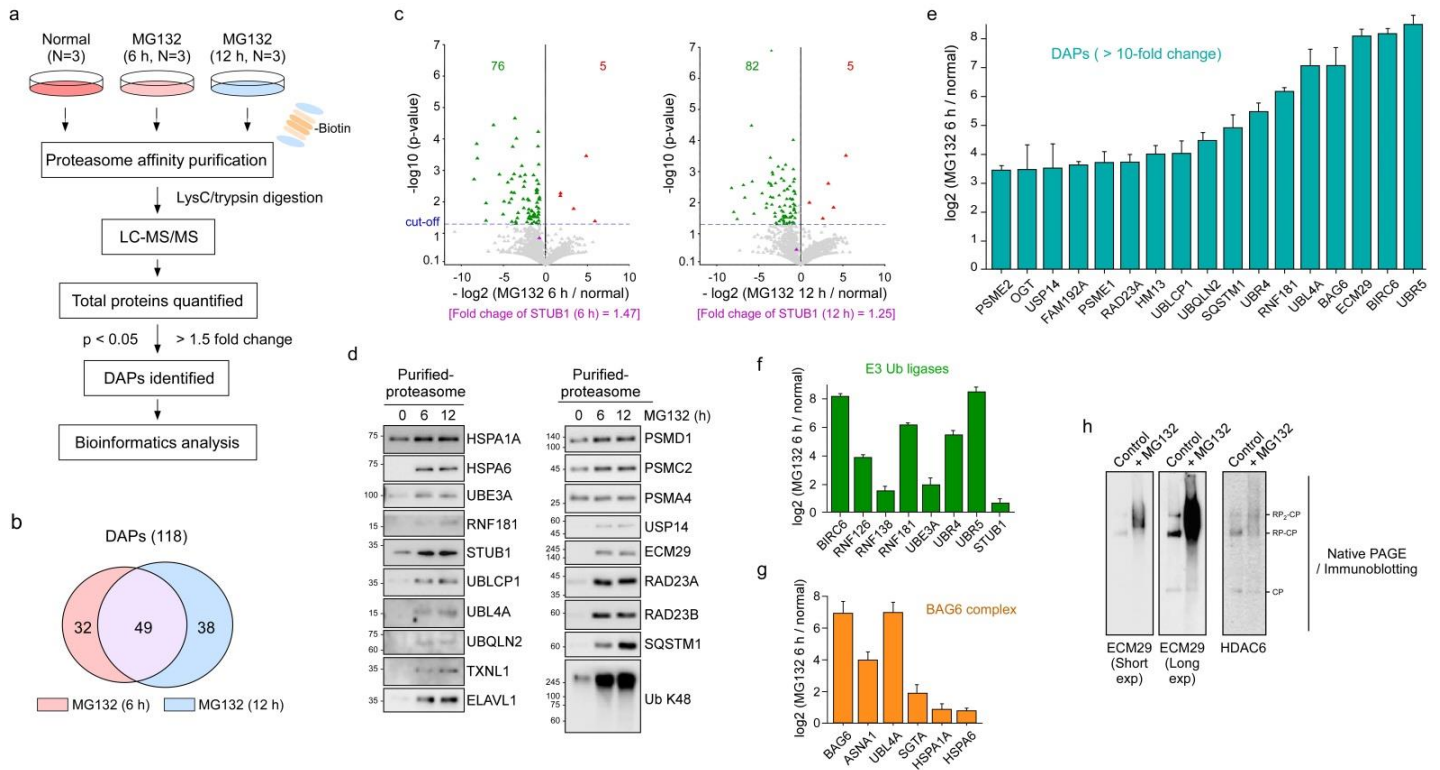
and PSMB5-positive aggresomes. n.s., no significance. **(b)** A549 cells were transfected with either 10 nM scrambled siRNA (siControl) or siRNA for silencing *HDAC6* (siHDAC6). Protein samples were collected 48 h post-transfection, separated into Triton-X-100-soluble and -insoluble fractions, and analyzed by SDS-PAGE/IB. **(c)** Quantitation of IFS results from Figs. 1f and 1i. A549 cells were incubated with either nocodazole (2 μ M) plus MG132 (5 μ M) for 12 h or siHDAC6 (20 nM for 48 h pretreatment) followed by MG132 treatment (5 μ M for additional 12 h). Each bar represents the mean (\pm SD) of three independent experiments with > 1,000 cells. ***, $p < 0.001$ (one-way ANOVA followed by the Bonferroni *post hoc* test). These data supplement Figs. 1f and 1i. **(d)** Quantitation of PSMA4 (*left*), PSMC2 (*middle*), and SQSTM1 (*right*) signals in Fig. 2a, normalized to those of endogenous β -actin. *, $p < 0.05$, **, $p < 0.01$, ***, $p < 0.001$, compared with 4 h washout points in each condition (one-way ANOVA followed by the Bonferroni *post hoc* test) **(e)** Colocalization of LAMP1 with PSMB5 was detected by IFS after treatment with MG132 (5 μ M, 12 h) and a washout in a normal medium, BafA1- or 3-methyladenine (3-MA)-containing medium, or amino acid-deficient (-AA) medium for 12 h. These data supplement Figs. 2b and 2c. Scale bars: 10 μ m. **(f)** As in (e), except that initial washout with normal media was performed for 8 h and then secondary washout was proceeded with media containing MG132 (5 μ M) or MG132 plus BafA1 (100 nM) for subsequent 4 h. **(g)** HeLa cells were transfected with siSQSTM1 for 24 h, treated with 5 μ M MG132 for 12 h, and then subjected to the washout with the normal medium or a BafA1 containing medium. IFS analysis was performed with anti-PSMB5 (green) and anti-SQSTM1 (red) antibodies.



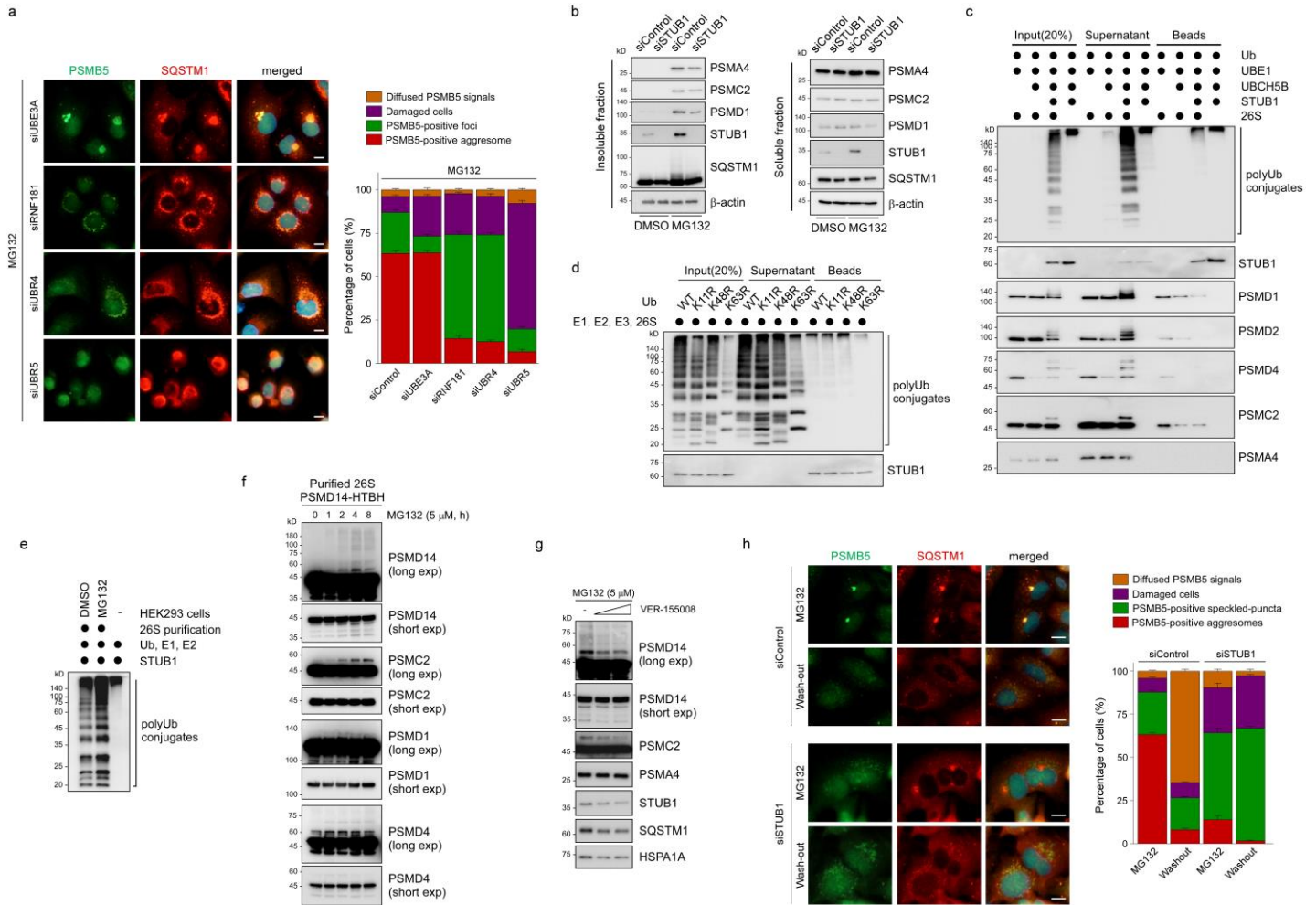
Supplementary Figure 5. Involvement of autophagy in the proteasome clearance and protective effect of aggresome formation in the cell. (a) The knockdown of autophagy genes resulted in delayed clearance of proteasome subunits in the insoluble fractions after the washout. A549 cells were transfected with siControl, siSQSTM1, and a combination of siATG5 and siATG7 for 48 h. Then, the cells were treated with MG132 (5 μ M, 12 h), followed by medium washout for 18 h. Detergent-insoluble fractions were analyzed by IB using CP and RP antibodies. (b) During the MG132 washout, an amino acid-deprived (-AA) medium, which induces overall cellular autophagy, was applied. Levels of various proteins such as PSMD1, PSMC2, PSMA4, PSMB6, SQSTM1, LC3, and β -actin in the detergent-soluble and -insoluble fractions were analyzed by SDS-PAGE/IB. (c) Cell viability was measured after 5 μ M MG132 treatment in the presence or absence of nocodazole (2 or 5 μ M). Values are presented as mean \pm SD (n = 3); *, $p < 0.01$ (one-way ANOVA with Bonferroni's multiple comparison test). N.S., no significance.



Supplementary Figure 6. Analysis of proteasomes in WCEs after MG132 treatment. (a) Sucrose-gradient ultracentrifugation of WCEs from HeLa cells with treatment with DMSO or MG132 (5 μ M, 12 h). Fractionized samples were analyzed by SDS-PAGE/IB with antibodies against various proteasome subunits such as PSMD1, PSMC2, and PSMA4, with SQSTM1 as controls. A significant proportion of the CP and RP subunits appeared to be shifted from the free form to the 26S species based on the sizes. (b) Size-exclusion chromatography of WCEs from A549 cells with treatment with DMSO or MG132 (5 μ M, 12 h). Immunoblotting analysis revealed proteasome subunits in the earlier fractions from the MG132-treated samples. Cofractionated molecular-weight standards such as blue dextran (2 MDa), thyroglobulin (669 kDa), and apoferritin (44.3 kDa) were indicated on top of the immunoblots.

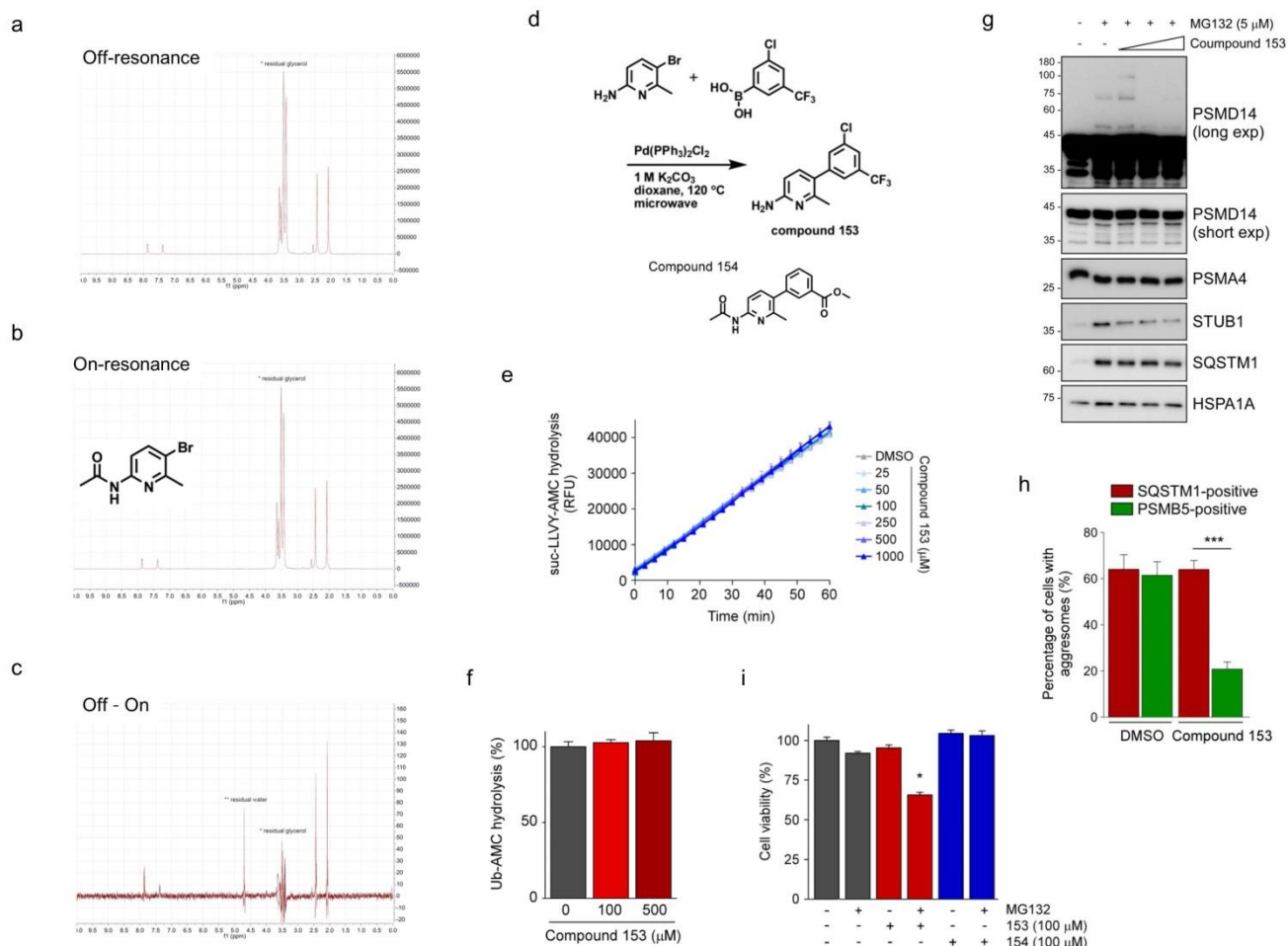


Supplementary Figure 7. Identification and validation of proteasome-interacting proteins with mass spectrometry (MS) based on intensity-based absolute quantification (iBAQ). (a) An overview of the LC-MS/MS approach, which was used for the quantitation of the inhibited-proteasome-interacting proteins by label-free methods. A total of 118 differentially associated proteins (DAPs) were identified in the cells treated with MG132 for 6 and 12 h, as compared to the cells under normal conditions. (b) A Venn diagram summary of the DAPs copurified with the inhibited proteasome. (c) The Volcano plot of DAPs. A threshold of the p value ($p < 0.05$) is shown as a blue dotted line. Log₂ ratios of purified proteasomes after treatment with MG132 to purified proteasomes under normal conditions are shown with gray (<1.5-fold change), green (>1.5-fold increase in purified proteasomes after proteasome inhibition), and red (>1.5-fold decrease in purified proteasomes after proteasome inhibition). (d) Immunoblotting analysis of the DAPs identified by iBAQ-MS. (e) The list of DAPs with more than 10-fold changes after 6 h of MG132 treatment, which includes E3 Ub ligases, proteasome modifiers, and Ub-like proteins. (f, g) Representative quantitation data comparing E3 Ub ligases (f) and the components of the BAG6 complex (g) after MG132 treatment. (h) Strong association of ECM29 and HDAC6 with the 26S proteasome was analyzed by non-denaturing (native) PAGE/IB of purified proteasomes.



Supplementary Figure 8. Critical role of STUB1 in the aggresomal segregation step of inhibited proteasomes. (a) Effects on aggresome formation when A549 cells were transfected siRNA constructs as indicated. The cells were analyzed by IFS with anti-PSMB5 (green) and anti-SQSTM1 (red) antibodies after MG132 treatment (5 μ M, 12 h). The columns and error bars in the quantitation based on the punctate morphology represent the mean and S.E.M. of three biological replicates. More than two hundred of the transfected cells were evaluated for proteasome positive aggregation patterns in each experiment. These data supplement Fig. 3a. (b) A549 cells were transfected with either 20 nM scrambled siRNA (siControl) or siRNA for silencing *STUB1* (siSTUB1) for 36 h and treated with MG132 (10 μ M for 12 h). Protein samples were collected, separated into Triton-X-100-soluble and -insoluble fractions, and analyzed by SDS-PAGE/IB. (c) *In vitro* polyubiquitylation of affinity-purified human proteasomes. The 26S proteasomes were and incubated with recombinant Ub, UBE1, UBE2D2, and GST-tagged STUB1 proteins in different combinations. GST-STUB1 was subsequently removed

using glutathione-agarose. The ubiquitylation of 26S proteasomes (Supernatants) and STUB1 (Beads) was monitored with SDS-PAGE/IB using anti-Ub antibodies. These data supplement Fig. 3c. **(d)** As in Fig. 3g, glutathione beads-bound GST-STUB1 was separated from the reaction products in the supernatants and subject to SDS-PAGE/IB using anti-Ub antibodies. **(e)** *In vitro* polyubiquitylation reactions were conducted with purified 26S proteasomes from the cells treated with DMSO or MG132 (5 μ M, 12 h) and used for the *in vitro* reaction with Ub, UBE1, UBE2D2, and STUB1. These data complement Fig. 3h. **(f)** *In vivo* ubiquitylation of proteasomes in HEK293 cells stably overexpressing biotin-tagged RP subunit PSMD14, which were treated with MG132 (5 μ M) for indicated time periods. Human proteasomes were affinity-purified from WCEs and then analyzed by SDS-PAGE/IB. **(g)** As in (f), except that cells were pre-treated with 0, 25, or 50 μ M of HSP70 inhibitor VER-155008 for 2 h, and then treated with MG132 (5 μ M) for additional 6h. SDS-PAGE/IB analysis revealed that *in vivo* ubiquitylation of PSMC2 and PSMD14 was delayed in the presence of VER-155008. **(h)** Delayed elimination of cytoplasmic puncta formed in *STUB1* knockdown cells after MG132 treatment (5 μ M, 12 h) and after subsequent washout (12 h). The cells were next analyzed by IFS with anti-PSMB5 (green) and anti-SQSTM1 (red) antibodies. The columns and error bars in the quantitation based on the punctate morphology represent the mean and S.E.M. of three biological replicates. More than two hundred of the transfected cells were evaluated for proteasome positive aggregation patterns in each experiment.



Supplementary Figure 9. Screening of STUB1-interacting fragments, and synthesis and biochemical analysis of compound 153. (a and b) Representative ^1H -NMR spectroscopic data for the screening of STUB1-interacting fragments. Our screening utilized a ligand-observed NMR assay monitoring differences in the ligand spectra upon interaction with STUB1 proteins. For saturation transfer difference (STD), NMR signals of STUB1 was selectively saturated by radio frequency (RF) irradiation (“Off” status, a) and this saturation was specifically transferred to the hit ligand (“On”, b). (c) The difference in proton spectra between “Off” and “On” status. Four lead fragments were identified from the primary and secondary screening. The chemical structure of the hit compound is shown. Peaks from residual glycerol (*) and residual water (**) in the screening buffer are indicated in the proton NMR spectra. (d) The fragment hits were utilized as *bona fide* starting points for further synthesis of lead compounds to target multiple segments of STUB1 proteins. The brief scheme for compound 153 synthesis is shown. Chemical structure of a structural control compound 154 is also shown. These data

complement Fig. 4a. **(e)** Assays of suc-LLVY-AMC hydrolysis were performed with purified human proteasomes with various concentrations of compound 153, which shows virtually no effect up to 1 mM. **(f)** Deubiquitinating activity of purified proteasomes was monitored by Ub-AMC hydrolysis assay with compound 153. **(g)** *In vivo* ubiquitylation of PSMD14 subunit was delayed with compound 153. Cells were pre-treated with 12.5, 25, or 50 μ M compound 153 for 2 h, and then treated with MG132 (5 μ M) for 6h. Human proteasomes were affinity-purified from WCEs and then analyzed by SDS-PAGE/IB. Notably, the amounts of proteasome-associating STUB1 decreased in the presence of compound 153. **(h)** Quantitation of A549 cells with PSMB5-positive (green) or SQSTM1-positive (red) aggresomes. Cells were treated with MG132 (5 μ M, 12 h) in the absence or presence of compound 153 (75 μ M, 12 h). Each bar represents the mean (\pm SD) of three independent experiments with > 1,000 cells. ***, $p < 0.001$ (two-tailed Student's t test). These data supplement Fig. 4e. **(i)** Assessment of cytotoxicity from the small molecules. Compound 153 and 154 were cotreated to A549 cells at 100 μ M concentration with 5 μ M MG132. After 12 h of the incubation, CellTiter-Glo bioluminometric cell viability assay was performed. Each data point is a mean \pm SD of three independent experiments.

SUPPLEMENTARY METHODS

Plasmids, antibodies, and reagents

Plasmids expressing HDAC6 and dynein were purchased from Addgene. Various plasmids encoding STUB1 were kindly provided by J. Song¹. The plasmid DNA was amplified with the Plasmid Midi Kit (GeneAll), according to the manufacturer's directions, and was stored at -20°C until use. Antibody sources and dilution factors were as follows: anti- β -actin (A1978, Sigma, 1/10,000), anti-Ub (clone P4D1, Santa Cruz Biotechnology, 1/5,000), anti-GAPDH (sc-32233, Santa Cruz Biotechnology, 1/1,000), anti-PSMA4 (PW8115, Enzo Life Science, 1/5,000), anti-PSMA3 (PW8110, Enzo Life Sciences, 1/3,000), anti-PSMB5 (PA1977, Invitrogen, 1/1,000), anti-PSMC2 (sc-166972, Santa Cruz Biotechnology, 1/1,000), anti-PSMD1 (sc-514809, Santa Cruz Biotechnology, 1/1,000), anti-PSMD14 (ab109123, Abcam, 1/1,000), anti-ADRM1 (ABS296-0100, Enzo Life Science, 1/1,000), anti-HDAC6 (MA5-25317, Invitrogen, 1/1,000), anti-ECM29 (PA3-035, Invitrogen, 1/250), anti-FLAG (F1804, Sigma, 1/3,000), anti-GST (MA4-004, Invitrogen, 1/1,000), anti-SQSTM1 (ab56416, Abcam, 1/10,000), anti-LC3 (L7543, Sigma, 1/2,000), anti-STUB1 (A301-572A, Bethyl Laboratories, 1/1,000), and anti-GFP antibody (Enogene, 1/5,000). Sources of major biochemical reagents were as follows: MG132, succ-LLVY-AMC (Bachem); PS341 (LC Laboratories); epoxomicin, Ub-AMC (Boston Biochem); carfilzomib (Cayman); ATP (Calbiochem); Coomassie Brilliant Blue R250 (Sigma). DMEM, RPMI, and EBSS media, fetal bovine serum (FBS), and phosphate-buffered saline (PBS; pH 7.4) were purchased from WelGENE.

Mammalian cell cultures and transient expression

Mammalian cells used in this study, including HEK293, HEK293-PSMB2-biotin, MEFs, and HeLa, CFTR- Δ F508-HeLa cells were grown in DMEM, whereas A549 cells were grown in RPMI 1640. All the culture media were supplemented with 10% of FBS, 100 U/mL penicillin, 100 $\mu\text{g}/\text{mL}$ streptomycin, and 2 mM L-glutamine. The cells were maintained in a humidified atmosphere containing 5% of CO_2 at 37°C . *STUB1*^{-/-} MEFs were established from homozygous *STUB1* null mice at embryonic day 12.5. Primary MEFs were then immortalized by transfecting Simian Virus 40 large T-antigen. For transient overexpression, cells were transfected with 1–2 μg of total plasmid DNA in a 6-well culture plate (>95% confluent or at a density of 10^6 cells/well) for 36–48 h using Lipofectamine 3000 (Invitrogen), according to the manufacturer's guidelines. For amino acid starvation, the growth medium was replaced with EBSS after two washes with PBS.

Immunofluorescence microscopy

For IFS analysis, cultured cells on a cover glass were fixed with 4% paraformaldehyde in PBS for 10 min. After that, the fixed cells were permeabilized with 0.5% (v/v) Triton X-100 in PBS, blocked with 2% BSA in PBS, and incubated with primary antibodies such as, for examples, the anti-SQSTM1 antibody (1:200 dilution) in the blocking solution for 1 h. Next, the cells were incubated for 40 min with Alexa Fluor 488– or Alexa Fluor 594–conjugated secondary antibodies diluted (1:1,000) for additional 1 h. The cells were then mounted with a 4',6'-diamidino-2-phenylindole (DAPI)-containing mounting solution (Abcam). Most of the fluorescent signals were monitored and captured using an Olympus fluorescence microscope (IX71) and images were processed using Adobe Photoshop CC. And confocal images were taken by laser scanning confocal microscope LSM 700 (Zeiss) under a 63x oil-immersion objective (c-Apochromat 63x/1.20 W Korr M27) at a definition of 1,024 x 1,024 pixels with the pinhole diameter adjusted to 1 AU. Then, images were analyzed by ZEN 2012 SP5 black edition image browser

(Release ver. 14.0.10.201). Within each figure, all images were captured using identical microscope settings and representative of the whole cell population.

Holotomography imaging

For RI imaging, cells were plated on 50 mm imaging dishes with a #1.5H glass coverslip bottom (TomoDish, Tomocube) and stabilized in a 37 °C incubator for 24 h to maintain a confluence of approximately 60%. After 12 h of Mg132 treatment, the cells were washed twice with PBS, followed by replacement of the medium with a fresh complete medium. The light scattered by the cells was transmitted through an objective lens (UPLASAPO 60XW, Olympus) and was then recorded by a CMOS camera (FL3-U3-13Y3M-C, FLIR Systems). The camera was synchronized with the digital micro-mirror device to record 49 holograms of the sample illuminated at different angles. By a phase-retrieval algorithm, the amplitude and phase images of the cells were retrieved from the obtained holograms.

Sphericity quantification

This analysis was performed with the TomoStudio software (ver. 2.7.30; Tomocube). The area of aggresomes corresponding to SQSTM1 antibody fluorescence was cropped, and the RI distribution of aggresomes was determined. Based on the threshold RI value, segmentation was performed using the Analysis tool in TomoStudio to create an iso-surface of the aggresomes. Volume and surface area of the iso-surface were used to calculate the sphericity of aggresomes. The protein concentration was also calculated in TomoStudio. The cytoplasmic protein concentrations are linearly proportional to their RI value via a constant called the RI increment.

Analysis of soluble and insoluble fractions

Cultured cells were washed with ice-cold PBS and lysed with either Triton X-100 buffer (200 mM KCl, 20 mM 4-[2-hydroxyethyl]-1-piperazineethanesulfonic acid-KOH pH 7.9, 1 mM MgCl₂, 1 mM EDTA, 1% of Triton X-100, and 10% of glycerol) or RIPA buffer (50 mM Tris-HCl pH 8, 1% of NP-40, 0.5% of deoxycholate, 0.1% of sodium dodecyl sulfate [SDS], and 150 mM NaCl), all supplemented with protease inhibitors. The lysates were then centrifuged at 16,000 × g for 30 min at 4 °C. The supernatants were designated as a detergent-soluble fraction. The pellets were washed with lysis buffer and resuspended in lysis buffer supplemented with 1% of SDS, then were sonicated for 10 s with a microtip sonicator, heated at 100 °C for 10 min, and were analyzed as a detergent-insoluble fraction. Equal volumes of each insoluble and soluble fraction were boiled for 10 min in SDS sample buffer and analyzed by IB.

RNA interference

The siRNAs were synthesized by Genolution. Using G-fectin (Genolution) or RNAiMAX (Invitrogen), siRNA was transfected into cells following the manufacturer's protocols. The final concentration of siRNA for the transfection was 20 nM. After 48 h of the transfection, 5 μM MG132 treatment for 12 h and MG132 washout were conducted. The following siRNAs were employed in this study: as a control (5'-CCUCGUGCCGUUCCAUCAGGUAGUU-3' sense, 5'-CUACCUGAUGGAACGGCAGGAGUU-3' antisense), for HDAC6 (5'-GAAACAACCCAGUACAUGAUU-3' sense, 5'-UCAUGUACUGGGUUGUUUCUU-3' antisense), for SQSTM1 (5'-GACAUCUUCGAAUCUACAUU-3' sense, 5'-UGUAGAUUCGGAAGAUGUCUU-3' antisense), for ATG5 (5'-GCUAUAUCAGGAUGAGAUUU-3' sense, 5'-UAUCUCAUCCUGAUUAUAGCUU-3' antisense), for ATG7 (5'-GCUACUUCUGCAAUGAUGUUU-3' sense, 5'-ACAUCAUUGCAGAAGUAGCUU-3' antisense), for STUB1 (5'-CGCUG

GUGGCCGUGUAUUAUU-3' plus 5'-CUUCGAAUCGCGAAGAAGAUU-3' sense, 5'-UAAUACACGGCCACCAGCGUU-3' plus 5'-UCUUCUUCGCGAUUCGAAGUU-3' antisense), for BIRC6 (5'-CCUAGUUGCUCUUAUUCUUUU-3' sense, 5'-AAGAAUAGGAGCAACUAGGUU-3' antisense), for UBE3A (5'-CAAGAAAGGCGCUAGAAUUUU-3' plus 5'-CAACUCCUGCUCUGAGAUUU-3' sense, 5'-AAUUCUAGCGCCUUUCUUGUU-3' plus 5'-UAUCUCAGAGCAGGAGUUUGUU-3' antisense), for RNF181 (5'-CACUGAUGACGACACUUAUUU-3' sense, 5'-AUAAGUGUCGUCAUCAGUGUU-3' antisense), for UBR4 (5'-CAACAUCUGCCCUUCAAAUUU-3' sense, 5'-AUUUGAAGGGCAGAUGUUGUU-3' antisense), and for UBR5 (5'-GCUUGAUGAGCCAUAUAGAAUU-3' sense, 5'-UUCUAAUGGCUCAUCAAGCUU-3' antisense).

Quantitative RT-PCR

Total RNA from cultured cells was isolated via the TRIzol Reagent (Invitrogen), followed by further purification by on-column DNase I treatment on RNeasy Mini-Columns (Qiagen). cDNA samples were prepared by reverse transcription with the Accupower RT-preMix (Bioneer). Then, quantitative RT-PCR reactions were carried out on a Rotor-Gene RG 3000 system (Corbett Research) with diluted cDNA and 10 pmol of target gene-specific primers. The SYBR qPCR master mixture (Kapa Biosystems) served as the reporter dye. Thermal cycling conditions included 95 °C for 3 min to allow for enzyme activation, followed by 40 cycles of 95 °C for 10 s, 53 °C for 15 s, and 72 °C for 30 s. The level of each mRNA was normalized to *GAPDH* levels of each cDNA sample, and the values were plotted as mean \pm SD of three independent experiments. The target gene-specific primer sequences were as follows: for PSMB5, forward 5'-ACTACGTGGACAGTGAAGGG-3' and reverse 5'-GGCATCTCTGTAGGTGGCTT-3'; for PSMD4, forward 5'-CTTCGTGTATCTATGGAA-3' and reverse 5'-TCATACTGCTTAGGTCAGG-3'; for PSMA7 forward 5'-AAGCAGCGTTATACGCAGAG-3' and reverse 5'-CATCAAAGTCGAAACCCACGAT-3'; for PSMA4, forward 5'-AGAAGTGGAGCAGTTGATCA-3' and reverse 5'-TCTCTGATTCTATTTATCCTTTTCT-3'; for PSMD4, forward 5'-AACAGTGAGTATATGCGGAATGG-3' and reverse 5'-ACTTCACAGTCATTAGCCAGTG-3'; for RSP27A, forward 5'-TCTCGACGAAGGCGACTAAT-3' and reverse 5'-TCGTGGTGGTGCTAAGAAAA-3'; for UBA52, forward 5'-AGGAGGGTATCCACCTGAC-3' and reverse 5'-CAGGGTGGACTCTTTCTGGA-3'; for UBC, forward 5'-CCTGGTGCTCCGTCTTAGAG-3' and reverse 5'-TTTCCAGCAAAGATCAACCT-3'; for UBB, forward 5'-TGCGTCTGAGAGGTGGTATG-3' and reverse 5'-GCCTTCACATTTTCGATGGT-3'; for SQSTM1, forward 5'-AAGCCGGGTGGGAATGTTG-3' and reverse 5'-CCTGAACAGTTATCCGACTCCAT-3'; for LC3, forward 5'-AACATGAGCGAGTTGGTCAAG-3' and reverse 5'-GCTCGTAGATGTCCGCGAT-3'; for ATG5, forward 5'-GCAAGCCAGACAGGAAAAAG-3' and reverse 5'-GACCTTCAGTGGTCCGGTAA-3'; for ATG12, forward 5'-CCCAGACCAAGAAGTTGGAA-3' and reverse 5'-GTCTCTTGCCACAAGCATCA-3'; and for GAPDH, forward 5'-GAGTCAACGGATTTGGTCGT-3' and reverse 5'-GACAAGCTTCCCGTTCTCAG-3'.

Purification of recombinant proteins and 26S human proteasomes

Recombinant proteins were purified as previously described^{1, 2}. Briefly, pGEX-4T-1-hSTUB1 was transfected into *Escherichia coli* BL21, and the resultant cultures were incubated at 37 °C until optical density at 600 nm (OD₆₀₀) reached 0.5. After addition of 0.2 mM isopropyl β -d-1-thiogalactopyranoside, cells were cultured overnight at 20 °C with agitation. The cells were resuspended in lysis buffer (50 mM NaH₂PO₄ pH 7.4, 300 mM NaCl, 20 mM β -mercaptoethanol, and 30% of glycerol) containing the

protease inhibitor cocktail and were lysed by sonication. After the lysate was centrifuged, the supernatant was incubated with Glutathione Sepharose (GE Healthcare) at 4 °C for 15 h. The resin was washed three times with washing buffer (lysis buffer with 0.2% of Triton X-100), then GST-hSTUB1 protein was eluted with 10 mM glutathione and concentrated on an Amicon ultracentrifugal filter (Millipore).

Human proteasome holoenzymes were isolated by affinity purification from a stable HEK293 cell line expressing biotin-tagged human PSMB2 as previously described with slight modifications². The cells were cultured in 15 cm culture dishes, harvested with lysis buffer (50 mM NaH₂PO₄ [pH 7.5], 100 mM NaCl, 10% of glycerol, 5 mM MgCl₂, 0.5% of NP-40, 5 mM ATP, and 1 mM dithiothreitol) containing protease inhibitors, and were homogenized in a Dounce homogenizer. After that, the lysates were centrifuged at 16,000 × g for 15 min at 4 °C. Next, the supernatants were incubated with BioMag Streptavidin resin (Qiagen) for 6 h at 4 °C. The beads were washed with lysis buffer and TEV buffer (50 mM Tris-HCl [pH 7.5], 1 mM ATP, and 10% of glycerol). The 26S proteasomes were eluted from the resin by incubation with TEV protease (Invitrogen) in TEV buffer containing 1 mM ATP for 1 h at 30 °C. Then, the eluted proteasomes were concentrated using Amicon ultracentrifugal filters.

Measurement of proteasome activity and deubiquitinating activity

Hydrolysis of fluorogenic peptide substrates suc-LLVY-AMC (Bachem) was quantified to determine the proteolytic activity of proteasomes. Briefly, the fluorogenic-peptide substrate hydrolysis assay was carried out with 10 µg of WCEs and 12.5 µM suc-LLVY-AMC. The reaction mixture contained 50 nM Tris-HCl pH 7.5, 1 mM EDTA, 1 mg/mL BSA, 1 mM ATP, and 1 mM DTT. Deubiquitinating activity was measured with hydrolysis of Ub-AMC (Boston Biochem). Proteasomal activity and deubiquitinating activity were monitored by measurement of free AMC fluorescence in a black 96-well plate on a TECAN Infinite m200 fluorometer.

Cell cycle analysis

After the treatment with either dimethyl sulfoxide (DMSO) or MG132 for various periods at several concentrations, the cells were collected by trypsinization. Each pellet was washed three times with cold PBS and fixed in 70% ethanol at 4 °C overnight. They were then centrifuged at 200 × g for 5 min at room temperature. After that, each cell pellet was resuspended in PBS and incubated with the DAPI/Triton X-100 staining solution and RNase A (50 µg/mL, Sigma) at room temperature for 30 min in the dark. The cells were next analyzed by flow cytometry (BD LSRFortessa) with UV light excitation at 340 to 380 nm. Data analysis was performed in the Flowjo software.

Assessment of cell viability

This property was assessed by the CellTiter-Glo Luminescent Cell Viability Assay (Promega) kit in accordance with the manufacturer's protocol. Briefly, cells were grown in black-wall/clear-bottom 96-well plates, treated with either MG132 (5 µM) or nocodazole (2 or 5 µM), and then luminescence substrates were added in the same volume as the cell culture medium. The mixture was incubated for 10 min at room temperature on a shaker, followed by luminescence measurement.

Nondenaturing gel electrophoresis

Native gel analysis of purified proteasomes or cell lysates was performed largely as described before³. Briefly, samples were resolved by native PAGE using NuPAGE 3-8% Tris-Acetate Protein Gels (Thermo Fisher) at 150 V for 3–4 h. Then proteins in the gel were directly analyzed by in-gel suc-

LLVY-AMC hydrolysis assay, or transferred to polyvinylidene difluoride membranes and subsequently immunoblotted for proteasome subunits and proteasome-interacting proteins.

LC-MS/MS analysis

LC-MS/MS analysis on a Q Exactive Plus Hybrid Quadrupole-Orbitrap mass spectrometer (Thermo Fisher Scientific) was performed as previously described⁴. Briefly, peptide samples were separated on a two-column system, consisting of a trap column and an analytical column (75 $\mu\text{m} \times 50 \text{ cm}$), with a 120 min gradient from 7% to 32% acetonitrile at 300 nL/min. Column temperature was maintained at 60 °C with a column heater. The MS/MS spectra were acquired at a resolution of 17,500 at $m/z \approx 200$ with 30% of normalized collision energy. The maximum ion injection time for the full scan and MS/MS scan was 20 and 100 ms, respectively. The obtained raw MS data were processed in MaxQuant version 1.5.3.1, which was also employed for postacquisition precursor m/z calibration, MS/MS spectrum peak picking, and peptide quantification⁵. The MS/MS spectra were subjected to searches in the Human UniProt protein sequence database by means of the Andromeda search engine. Mass tolerance for precursor ions and MS/MS ions was set to 6 and 20 ppm, respectively. The global false discovery rate for the peptide, protein, and modification level was set to 1%.

For label-free quantification of proteasome-associated proteins, the iBAQ algorithm⁶ was utilized as part of the MaxQuant platform. Briefly, the iBAQ values, which are the raw intensities divided by the number of theoretical peptides and proportional to the molar quantities of the proteins, were normalized to the average values of 14 CP subunits (PSMA1 to PSMA7 and PSMB1 to PSMB7). A DAP was considered statistically significant if its fold change was ≥ 1.5 and if it had a P value < 0.05 . For a comparison of proteomes, two-sided *t* tests were performed with a significance level of 5%. All statistical analyses were performed in the Perseus software.

Size exclusion chromatography and sucrose-gradient ultracentrifugation

Cell lysates were centrifuged twice at $18,000 \times g$ for 30 min at 4 °C. The final supernatant of each condition was loaded (11 mg by protein) onto a column and eluted with proteasome SEC buffer (50 mM NaH_2PO_4 [pH 7.5], 10 mM NaCl, 5 mM MgCl_2 , 5 mM ATP, and 1 mM DTT). SEC was carried out on a Superose 6 Increase 10/300 GL column by fast protein liquid chromatography (Ä KTA; GE Healthcare); 0.25 mL fractions were collected, and 10% glycerol was added to each fraction. Each standard was prepared at a concentration of 3 mg/mL in PBS, and the standards were loaded onto a column simultaneously. Blue dextran (M_r : 2,000,000) peaked in fraction 36, thyroglobulin (M_r : 669,000) peaked in fraction 54, and ovalbumin (M_r : 44,000) in fraction 70.

For sucrose-gradient ultracentrifugation, HeLa cells were added by 15 mL of warm PBS containing 100 $\mu\text{g/mL}$ cycloheximide and kept for 15 min to immobilize ribosomes on mRNAs. After that, the cell extracts were resuspended with 1 mL of lysis buffer (50 mM 3-[N-morpholino]propanesulfonic acid, 15 mM MgCl_2 , 150 mM NaCl, 100 $\mu\text{g/mL}$ cycloheximide, 0.5% of Triton X-100, 1 mg/mL heparin, 0.2 U/ μL RNase inhibitor, 2 mM phenylmethylsulfonyl fluoride, and 1 mM benzamidine) and centrifuged. After harvesting, the soluble fraction was loaded on top of a pre-established sucrose gradient (10 mL, 10–50%) and centrifuged at 36,000 rpm in a Beckman SW-41 Ti rotor for 2 h at 4 °C. After that, gradients were fractionated and collected using the ISCO tube piercer (Brandel) and fraction collector (Bio-Rad) according to absorbance at 254 nm.

***In vitro* ubiquitylation of purified proteasomes**

For ubiquitylation of the purified proteasome, 50 μM ubiquitin (Boston Biochem) or mutant ubiquitin (K11R, K48R, or K63R; Enzo), 150 nM UBE1 (UBPBio), and 1 μM UBE2D2 (Boston Biochem) were

incubated for 10 min at room temperature in 1× ATP buffer (50 mM Tris-HCl [pH 7.4], 100 mM NaCl, 10% of glycerol, 5 mM DTT, 2 mM ATP, and 10 mM MgCl₂). Then, 500 nM GST-STUB1 and 60 nM purified proteasome were added, and total reaction volume was brought to the necessary value with reaction buffer (50 mM Tris-HCl pH 7.4, 100 mM NaCl, and 10% of glycerol). The reactions were allowed to proceed for 4 h at 37 °C. The reactions were stopped by the addition of SDS sample buffer and then loaded on a gel for IB analysis.

To remove GST-STUB1 from the *in vitro* ubiquitylation reactions of the proteasome, reaction products were incubated with pre-equilibrated glutathione-sepharose 4B beads (GE Healthcare) with gentle rotation at room temperature for 2 h. Then, the beads and the supernatant were separated by brief centrifugation at 600 × *g*. The beads were washed 3 times with Ub reaction buffer (50 mM Tris-HCl [pH 7.4], 100 mM NaCl, and 10% glycerol). Proteins bound to the beads were resuspended in 2 × SDS sample buffer, boiled for 10 min, and loaded on a gel for IB analysis.

¹H ligand-observed STD NMR screening

For NMR screening, the protein buffer was exchanged by ultrafiltration with a solution of 50 mM NaCl, 10 mM potassium phosphate, and 0.1 mM NaN₃ (pH 7.0). In order to identify compounds that can bind to STUB1 protein, we employed ¹H ligand-observed NMR screening methods like the Saturation-Transfer Difference (STD) experiment with 2nd Generation BIONET Premium Fragment Library. Each fragment was stocked as 100 mM DMSO-*d*₆ solution. The STD NMR experiments were carried out at 293 K on an 800 MHz Bruker NMR spectrometer equipped with a cryoprobe. Preliminary STD NMR screenings were performed with a mixture of five different fragments. NMR samples (500 μL) for STD experiments were prepared with 1 mM of each fragment in 50 mM NaCl, 10 mM potassium phosphate, and 0.1 mM NaN₃ at pH 7.0 in D₂O either in the presence or absence of 1 μM of STUB1. For fragments presenting the binding potential, secondary STD NMR experiments were carried out with the single fragment itself to confirm the binding.

Synthesis of compound 153

To a solution of 5-bromo-6-methylpyridin-2-amine (100 mg, 0.54 mmol) in dioxane (7.1 mL) were added (3-chloro-5-(trifluoromethyl)phenyl)boronic acid (100 mg, 0.45 mmol) and 1 M aqueous solution of potassium carbonate (1.78 mL) at ambient temperature in a microwave vial. The resulting suspension was purged with nitrogen for 3 min, and bis(triphenylphosphine)palladium(II) dichloride (31.6 mg, 0.045 mmol) was added and the microwave vial was sealed with a microwave cap. Then, microwave was applied to the mixture at 120 °C for 3 h. The mixture was cooled down, diluted with ethyl acetate, and washed with water. The organic layer was dried with magnesium sulfate, filtered, and concentrated *in vacuo*. The residue was purified by preparative thin layer column chromatography (50% ethyl acetate-hexanes) to provide 5-(3-chloro-5-(trifluoromethyl)phenyl)-6-methylpyridin-2-amine (LSM153). ¹H-NMR (400 MHz, DMSO-*d*₆): δ 7.78 (s, 1H), 7.72 (s, 1H), 7.62 (s, 1H), 7.33 (d, 1H, *J* = 8.0 Hz), 6.37 (d, 1H, *J* = 8.0 Hz), 6.11 (s, 2H), 2.25 (s, 3H). (30 mg; yield 23.5%).

SUPPLEMENTARY REFERENCES

1. Seo, J. *et al.* CHIP controls necroptosis through ubiquitylation- and lysosome-dependent degradation of RIPK3. *Nat Cell Biol* **18**, 291-302 (2016).
2. Han, D.H. *et al.* Direct cellular delivery of human proteasomes to delay tau aggregation. *Nat Commun* **5**, 5633 (2014).
3. Choi, W.H. *et al.* Open-gate mutants of the mammalian proteasome show enhanced ubiquitin-conjugate degradation. *Nat Commun* **7**, 10963 (2016).
4. Han, D., Jin, J., Woo, J., Min, H. & Kim, Y. Proteomic analysis of mouse astrocytes and their secretome by a combination of FASP and StageTip-based, high pH, reversed-phase fractionation. *Proteomics* **14**, 1604-1609 (2014).
5. Tyanova, S. *et al.* The Perseus computational platform for comprehensive analysis of (prote)omics data. *Nat Methods* **13**, 731-740 (2016).
6. Schwanhaussner, B. *et al.* Global quantification of mammalian gene expression control. *Nature* **473**, 337-342 (2011).

SUPPLEMENTARY TABLE

Supplementary Table 1. (a) All the proteins identified by iBAQ-MS. (b) Normalized quantities of the identified proteins based on the levels of CP subunits. (c) Proteins differentially associated with proteasomes after 6 h MG132 treatment. (d) Proteins differentially associated with proteasomes after 12 h MG132 treatment. Proteomic raw data are available via ProteomeXchange with identifier PXD019193.

P04033		CAD-binding protein alpha chain	CBPA	0	0	0	0	0	0	0	77445
P04034		3-hydroxy-3-methylglutaryl-coenzyme A reductase	HMGCR	0	0	0	0	103710	862470	515600	387310
P04040		Catalase	CAT	0	0	0	0	0	0	0	58065
P04047		Fructose-bisphosphate aldolase A	ALDOA	131420000	120700000	8492900	126340000	38623000	42412000	68600000	48600000
P104048		Osmithine aminotransferase, mitochondrial	OAT	4586500	5770000	0	5277800	1274500	1154100	2875000	2875000
P104049		Tubulin beta-4A chain	TUBB4A	0	0	0	0	0	0	0	0
P104050		Glyceroldehyde 3-phosphate dehydrogenase	GAPDH	6195500	8792000	2421000	9150800	1834000	20617000	48629000	48629000
P104051		Alpha-amylase 2B	AMY2B	4278200	0	0	0	0	0	0	0
P104052		Heat shock protein beta 1	HSPB1	2713400	2713400	1977800	2074100	1066500	570000	570000	570000
P104053		Dolichyl-diphosphooligosaccharide- protein glycosyltransferase subunit 1	DPN1	541710	305000	0	0	168210	203970	330810	330810
P104054		Dolichyl-diphosphooligosaccharide- protein glycosyltransferase subunit 2	DPN2	1141300	765400	448100	0	844800	0	0	0
P104055		Coenzyme nucleotide-binding protein G0 subunit alpha 2	GNAL2	2182000	0	666280	9321200	1815800	1814100	9333200	9333200
P09876		Histone H2A type 1-Histone H2A type 1	H2A1	8289100	172220000	0	54629000	19577000	8783000	13668000	13668000
P09877		Histone H2A type 2-Histone H2A type 2	H2A2	8289100	172220000	0	54629000	19577000	8783000	13668000	13668000
P09878		Histone H2A type 3-Histone H2A type 3	H2A3	8289100	172220000	0	54629000	19577000	8783000	13668000	13668000
P09879		Histone H2A type 4-Histone H2A type 4	H2A4	8289100	172220000	0	54629000	19577000	8783000	13668000	13668000
P09880		Histone H2A type 5-Histone H2A type 5	H2A5	8289100	172220000	0	54629000	19577000	8783000	13668000	13668000
P09881		Histone H2A type 6-Histone H2A type 6	H2A6	8289100	172220000	0	54629000	19577000	8783000	13668000	13668000
P09882		Histone H2A type 7-Histone H2A type 7	H2A7	8289100	172220000	0	54629000	19577000	8783000	13668000	13668000
P09883		Histone H2A type 8-Histone H2A type 8	H2A8	8289100	172220000	0	54629000	19577000	8783000	13668000	13668000
P09884		Histone H2A type 9-Histone H2A type 9	H2A9	8289100	172220000	0	54629000	19577000	8783000	13668000	13668000
P09885		Histone H2A type 10-Histone H2A type 10	H2A10	8289100	172220000	0	54629000	19577000	8783000	13668000	13668000
P09886		Histone H2A type 11-Histone H2A type 11	H2A11	8289100	172220000	0	54629000	19577000	8783000	13668000	13668000
P09887		Histone H2A type 12-Histone H2A type 12	H2A12	8289100	172220000	0	54629000	19577000	8783000	13668000	13668000
P09888		Histone H2A type 13-Histone H2A type 13	H2A13	8289100	172220000	0	54629000	19577000	8783000	13668000	13668000
P09889		Histone H2A type 14-Histone H2A type 14	H2A14	8289100	172220000	0	54629000	19577000	8783000	13668000	13668000
P09890		Histone H2A type 15-Histone H2A type 15	H2A15	8289100	172220000	0	54629000	19577000	8783000	13668000	13668000
P09891		Histone H2A type 16-Histone H2A type 16	H2A16	8289100	172220000	0	54629000	19577000	8783000	13668000	13668000
P09892		Histone H2A type 17-Histone H2A type 17	H2A17	8289100	172220000	0	54629000	19577000	8783000	13668000	13668000
P09893		Histone H2A type 18-Histone H2A type 18	H2A18	8289100	172220000	0	54629000	19577000	8783000	13668000	13668000
P09894		Histone H2A type 19-Histone H2A type 19	H2A19	8289100	172220000	0	54629000	19577000	8783000	13668000	13668000
P09895		Histone H2A type 20-Histone H2A type 20	H2A20	8289100	172220000	0	54629000	19577000	8783000	13668000	13668000
P09896		Histone H2B type 1-Histone H2B type 1	H2B1	1714900	5704000	0	1667500	2211000	978480	2211000	978480
P09897		Histone H2B type 2-Histone H2B type 2	H2B2	1714900	5704000	0	1667500	2211000	978480	2211000	978480
P09898		Histone H2B type 3-Histone H2B type 3	H2B3	1714900	5704000	0	1667500	2211000	978480	2211000	978480
P09899		Histone H2B type 4-Histone H2B type 4	H2B4	1714900	5704000	0	1667500	2211000	978480	2211000	978480
P09900		Histone H2B type 5-Histone H2B type 5	H2B5	1714900	5704000	0	1667500	2211000	978480	2211000	978480
P09901		Histone H2B type 6-Histone H2B type 6	H2B6	1714900	5704000	0	1667500	2211000	978480	2211000	978480
P09902		Histone H2B type 7-Histone H2B type 7	H2B7	1714900	5704000	0	1667500	2211000	978480	2211000	978480
P09903		Histone H2B type 8-Histone H2B type 8	H2B8	1714900	5704000	0	1667500	2211000	978480	2211000	978480
P09904		Histone H2B type 9-Histone H2B type 9	H2B9	1714900	5704000	0	1667500	2211000	978480	2211000	978480
P09905		Histone H2B type 10-Histone H2B type 10	H2B10	1714900	5704000	0	1667500	2211000	978480	2211000	978480
P09906		Histone H2B type 11-Histone H2B type 11	H2B11	1714900	5704000	0	1667500	2211000	978480	2211000	978480
P09907		Histone H2B type 12-Histone H2B type 12	H2B12	1714900	5704000	0	1667500	2211000	978480	2211000	978480
P09908		Histone H2B type 13-Histone H2B type 13	H2B13	1714900	5704000	0	1667500	2211000	978480	2211000	978480
P09909		Histone H2B type 14-Histone H2B type 14	H2B14	1714900	5704000	0	1667500	2211000	978480	2211000	978480
P09910		Histone H2B type 15-Histone H2B type 15	H2B15	1714900	5704000	0	1667500	2211000	978480	2211000	978480
P09911		Histone H2B type 16-Histone H2B type 16	H2B16	1714900	5704000	0	1667500	2211000	978480	2211000	978480
P09912		Histone H2B type 17-Histone H2B type 17	H2B17	1714900	5704000	0	1667500	2211000	978480	2211000	978480
P09913		Histone H2B type 18-Histone H2B type 18	H2B18	1714900	5704000	0	1667500	2211000	978480	2211000	978480
P09914		Histone H2B type 19-Histone H2B type 19	H2B19	1714900	5704000	0	1667500	2211000	978480	2211000	978480
P09915		Histone H2B type 20-Histone H2B type 20	H2B20	1714900	5704000	0	1667500	2211000	978480	2211000	978480
P09916		Histone H2B type 21-Histone H2B type 21	H2B21	1714900	5704000	0	1667500	2211000	978480	2211000	978480
P09917		Histone H2B type 22-Histone H2B type 22	H2B22	1714900	5704000	0	1667500	2211000	978480	2211000	978480
P09918		Histone H2B type 23-Histone H2B type 23	H2B23	1714900	5704000	0	1667500	2211000	978480	2211000	978480
P09919		Histone H2B type 24-Histone H2B type 24	H2B24	1714900	5704000	0	1667500	2211000	978480	2211000	978480
P09920		Histone H2B type 25-Histone H2B type 25	H2B25	1714900	5704000	0	1667500	2211000	978480	2211000	978480
P09921		Histone H2B type 26-Histone H2B type 26	H2B26	1714900	5704000	0	1667500	2211000	978480	2211000	978480
P09922		Histone H2B type 27-Histone H2B type 27	H2B27	1714900	5704000	0	1667500	2211000	978480	2211000	978480
P09923		Histone H2B type 28-Histone H2B type 28	H2B28	1714900	5704000	0	1667500	2211000	978480	2211000	978480
P09924		Histone H2B type 29-Histone H2B type 29	H2B29	1714900	5704000	0	1667500	2211000	978480	2211000	978480
P09925		Histone H2B type 30-Histone H2B type 30	H2B30	1714900	5704000	0	1667500	2211000	978480	2211000	978480
P09926		Histone H2B type 31-Histone H2B type 31	H2B31	1714900	5704000	0	1667500	2211000	978480	2211000	978480
P09927		Histone H2B type 32-Histone H2B type 32	H2B32	1714900	5704000	0	1667500	2211000	978480	2211000	978480
P09928		Histone H2B type 33-Histone H2B type 33	H2B33	1714900	5704000	0	1667500	2211000	978480	2211000	978480
P09929		Histone H2B type 34-Histone H2B type 34	H2B34	1714900	5704000	0	1667500	2211000	978480	2211000	978480
P09930		Histone H2B type 35-Histone H2B type 35	H2B35	1714900	5704000	0	1667500	2211000	978480	2211000	978480
P09931		Histone H2B type 36-Histone H2B type 36	H2B36	1714900	5704000	0	1667500	2211000	978480	2211000	978480
P09932		Histone H2B type 37-Histone H2B type 37	H2B37	1714900	5704000	0	1667500	2211000	978480	2211000	978480
P09933		Histone H2B type 38-Histone H2B type 38	H2B38	1714900	5704000	0	1667500	2211000	978480	2211000	978480
P09934		Histone H2B type 39-Histone H2B type 39	H2B39	1714900	5704000	0	1667500	2211000	978480	2211000	978480
P09935		Histone H2B type 40-Histone H2B type 40	H2B40	1714900	5704000	0	1667500	2211000	978480	2211000	978480
P09936		Histone H2B type 41-Histone H2B type 41	H2B41	1714900	5704000	0	1667500	2211000	978480	2211000	978480
P09937		Histone H2B type 42-Histone H2B type 42	H2B42	1714900	5704000	0	1667500	2211000	978480	2211000	978480
P09938		Histone H2B type 43-Histone H2B type 43	H2B43	1714900	5704000	0	1667500	2211000	978480	2211000	978480
P09939		Histone H2B type 44-Histone H2B type 44	H2B44	1714900	5704000	0	1667500	2211000	978480	2211000	978480
P09940		Histone H2B type 45-Histone H2B type 45	H2B45	1714900	5704000	0	1667500	2211000	978480	2211000	978480
P09941		Histone H2B type 46-Histone H2B type 46	H2B46	1714900	5704000	0	1667500	2211000	978480	2211000	978480
P09942		Histone H2B type 47-Histone H2B type 47	H2B47	1714900	5704000	0	1667500	2211000	978480	2211000	978480
P09943		Histone H2B type 48-Histone H2B type 48	H2B48	1714900	5704000	0	1667500	2211000	978480	2211000	978480
P09944		Histone H2B type 49-Histone H2B type 49	H2B49	1714900	5704000	0	1667500	2211000	978480	2211000	978480
P09945		Histone H2B type 50									

Q2016		Translational activator GCV1	GCN1L1	15966	0	0	23890	0	0	0
Q2017	Q2017	Nuclear pore complex protein Nup55	NUP55	24550	321500	454440	439700	370100	291400	291400
Q2065		28S ribosomal protein S31, mitochondrial	MRPS31	419670	0	0	40220	0	0	341400
Q2068	Q2068	Acidic leucine-rich nuclear phosphoprotein 32 family member B	ANP32B	1772000	2462000	6617700	18613000	30150000	7317800	8942700
Q2071	Q2071	Actin-related protein 23, cytoskeletal 1A	ARPC1A	1366500	0	0	130700	1302000	2954000	0
Q20769		Histone deacetylase 2, histone deacetylase 1	HDAC2,HDAC1	1599900	1494800	24396	5113100	2531001	1103700	1738100
Q2077	Q2077	Synapsin	SYNAP	73846	0	0	167900	0	0	640190
Q20820		Gamma-glutamyl hydrolase	GGH	0	294510	0	686800	0	0	0
Q20828		Coronin-2A	COR2A	46810	0	0	0	0	16681	48238
Q2083	Q2083	DNA repair protein RAD50	RAD50	38054	38054	56662	2461010	1411200	184880	1411200
Q20900	Q20900	Regulator of nonsense transcripts 1	RNT1	1400700	65470	138140	1075700	181180	31990	31990
Q20913	Q20913	COPII signalosome complex subunit 5	COPI1	154840	108500	0	222900	54350	1170200	80770
Q20917		G patch domain and KOW motif-containing protein	GPWOW	64410	0	0	2100	0	38130	0
Q20924	Q20924	Far upstream element-binding protein 2	KHSBP	1256600	532800	1193700	1625700	376990	3025200	942620
Q20925	Q20925	Transcription factor 12	TNFR1	201600	99368	0	605800	0	340700	0
Q20925	Q20925	Ubiquitin carboxyl-terminal hydrolase 13	UBP13	0	0	0	245130	0	0	0
Q20938	Q20938	Probable ubiquitin carboxyl-terminal hydrolase FAX-X	USP9X	38154	38074	0	161900	0	99715	147680
Q20939	Q20939	Ubiquitin carboxyl-terminal hydrolase 13, ubiquitin carboxyl-terminal hydrolase	USP7	65510	0	141000	2160200	56382	203660	118500
Q20940		Protein RING1B	RING1B	3233300	3233300	3391000	4132700	2500000	913300	4423700
Q20948		Protein RING1A	RING1A	3233300	3233300	3391000	4132700	2500000	913300	4423700
Q20952	Q20952	Ubiquitin-conjugating enzyme E2, E2UBiquitin-conjugating enzyme E2	UBE2E,UBE2E2	396960	246480	0	413600	0	466800	2780700
Q20953		Protein RING1B	RING1B	3233300	3233300	3391000	4132700	2500000	913300	4423700
Q20953	Q20953	Protein RING1A	RING1A	3233300	3233300	3391000	4132700	2500000	913300	4423700
Q20953	Q20953	Protein RING1B	RING1B	3233300	3233300	3391000	4132700	2500000	913300	4423700
Q20953	Q20953	Protein RING1A	RING1A	3233300	3233300	3391000	4132700	2500000	913300	4423700
Q20953	Q20953	Protein RING1B	RING1B	3233300	3233300	3391000	4132700	2500000	913300	4423700
Q20953	Q20953	Protein RING1A	RING1A	3233300	3233300	3391000	4132700	2500000	913300	4423700
Q20953	Q20953	Protein RING1B	RING1B	3233300	3233300	3391000	4132700	2500000	913300	4423700
Q20953	Q20953	Protein RING1A	RING1A	3233300	3233300	3391000	4132700	2500000	913300	4423700
Q20953	Q20953	Protein RING1B	RING1B	3233300	3233300	3391000	4132700	2500000	913300	4423700
Q20953	Q20953	Protein RING1A	RING1A	3233300	3233300	3391000	4132700	2500000	913300	4423700
Q20953	Q20953	Protein RING1B	RING1B	3233300	3233300	3391000	4132700	2500000	913300	4423700
Q20953	Q20953	Protein RING1A	RING1A	3233300	3233300	3391000	4132700	2500000	913300	4423700
Q20953	Q20953	Protein RING1B	RING1B	3233300	3233300	3391000	4132700	2500000	913300	4423700
Q20953	Q20953	Protein RING1A	RING1A	3233300	3233300	3391000	4132700	2500000	913300	4423700
Q20953	Q20953	Protein RING1B	RING1B	3233300	3233300	3391000	4132700	2500000	913300	4423700
Q20953	Q20953	Protein RING1A	RING1A	3233300	3233300	3391000	4132700	2500000	913300	4423700
Q20953	Q20953	Protein RING1B	RING1B	3233300	3233300	3391000	4132700	2500000	913300	4423700
Q20953	Q20953	Protein RING1A	RING1A	3233300	3233300	3391000	4132700	2500000	913300	4423700
Q20953	Q20953	Protein RING1B	RING1B	3233300	3233300	3391000	4132700	2500000	913300	4423700
Q20953	Q20953	Protein RING1A	RING1A	3233300	3233300	3391000	4132700	2500000	913300	4423700
Q20953	Q20953	Protein RING1B	RING1B	3233300	3233300	3391000	4132700	2500000	913300	4423700
Q20953	Q20953	Protein RING1A	RING1A	3233300	3233300	3391000	4132700	2500000	913300	4423700
Q20953	Q20953	Protein RING1B	RING1B	3233300	3233300	3391000	4132700	2500000	913300	4423700
Q20953	Q20953	Protein RING1A	RING1A	3233300	3233300	3391000	4132700	2500000	913300	4423700
Q20953	Q20953	Protein RING1B	RING1B	3233300	3233300	3391000	4132700	2500000	913300	4423700
Q20953	Q20953	Protein RING1A	RING1A	3233300	3233300	3391000	4132700	2500000	913300	4423700
Q20953	Q20953	Protein RING1B	RING1B	3233300	3233300	3391000	4132700	2500000	913300	4423700
Q20953	Q20953	Protein RING1A	RING1A	3233300	3233300	3391000	4132700	2500000	913300	4423700
Q20953	Q20953	Protein RING1B	RING1B	3233300	3233300	3391000	4132700	2500000	913300	4423700
Q20953	Q20953	Protein RING1A	RING1A	3233300	3233300	3391000	4132700	2500000	913300	4423700
Q20953	Q20953	Protein RING1B	RING1B	3233300	3233300	3391000	4132700	2500000	913300	4423700
Q20953	Q20953	Protein RING1A	RING1A	3233300	3233300	3391000	4132700	2500000	913300	4423700
Q20953	Q20953	Protein RING1B	RING1B	3233300	3233300	3391000	4132700	2500000	913300	4423700
Q20953	Q20953	Protein RING1A	RING1A	3233300	3233300	3391000	4132700	2500000	913300	4423700
Q20953	Q20953	Protein RING1B	RING1B	3233300	3233300	3391000	4132700	2500000	913300	4423700
Q20953	Q20953	Protein RING1A	RING1A	3233300	3233300	3391000	4132700	2500000	913300	4423700
Q20953	Q20953	Protein RING1B	RING1B	3233300	3233300	3391000	4132700	2500000	913300	4423700
Q20953	Q20953	Protein RING1A	RING1A	3233300	3233300	3391000	4132700	2500000	913300	4423700
Q20953	Q20953	Protein RING1B	RING1B	3233300	3233300	3391000	4132700	2500000	913300	4423700
Q20953	Q20953	Protein RING1A	RING1A	3233300	3233300	3391000	4132700	2500000	913300	4423700
Q20953	Q20953	Protein RING1B	RING1B	3233300	3233300	3391000	4132700	2500000	913300	4423700
Q20953	Q20953	Protein RING1A	RING1A	3233300	3233300	3391000	4132700	2500000	913300	4423700
Q20953	Q20953	Protein RING1B	RING1B	3233300	3233300	3391000	4132700	2500000	913300	4423700
Q20953	Q20953	Protein RING1A	RING1A	3233300	3233300	3391000	4132700	2500000	913300	4423700
Q20953	Q20953	Protein RING1B	RING1B	3233300	3233300	3391000	4132700	2500000	913300	4423700
Q20953	Q20953	Protein RING1A	RING1A	3233300	3233300	3391000	4132700	2500000	913300	4423700
Q20953	Q20953	Protein RING1B	RING1B	3233300	3233300	3391000	4132700	2500000	913300	4423700
Q20953	Q20953	Protein RING1A	RING1A	3233300	3233300	3391000	4132700	2500000	913300	4423700
Q20953	Q20953	Protein RING1B	RING1B	3233300	3233300	3391000	4132700	2500000	913300	4423700
Q20953	Q20953	Protein RING1A	RING1A	3233300	3233300	3391000	4132700	2500000	913300	4423700
Q20953	Q20953	Protein RING1B	RING1B	3233300	3233300	3391000	4132700	2500000	913300	4423700
Q20953	Q20953	Protein RING1A	RING1A	3233300	3233300	3391000	4132700	2500000	913300	4423700
Q20953	Q20953	Protein RING1B	RING1B	3233300	3233300	3391000	4132700	2500000	913300	4423700
Q20953	Q20953	Protein RING1A	RING1A	3233300	3233300	3391000	4132700	2500000	913300	4423700
Q20953	Q20953	Protein RING1B	RING1B	3233300	3233300	3391000	4132700	2500000	913300	4423700
Q20953	Q20953	Protein RING1A	RING1A	3233300	3233300	3391000	4132700	2500000	913300	4423700
Q20953	Q20953	Protein RING1B	RING1B	3233300	3233300	3391000	4132700	2500000	913300	4423700
Q20953	Q20953	Protein RING1A	RING1A	3233300	3233300	3391000	4132700	2500000	913300	4423700
Q20953	Q20953	Protein RING1B	RING1B	3233300	3233300	3391000	4132700	2500000	913300	4423700
Q20953	Q20953	Protein RING1A	RING1A	3233300	3233300	3391000	4132700	2500000	913300	4423700
Q20953	Q20953	Protein RING1B	RING1B	3233300	3233300	3391000	4132700	2500000	913300	4423700
Q20953	Q20953	Protein RING1A	RING1A	3233300	3233300	3391000	4132700	2500000	913300	4423700
Q20953	Q20953	Protein RING1B	RING1B	3233300	3233300	3391000	4132700	2500000	913300	4423700
Q20953	Q20953	Protein RING1A	RING1A	3233300	3233300	3391000	4132700	2500000	913300	4423700
Q20953	Q20953	Protein RING1B	RING1B	3233300	3233300	3391000	4132700	2500000	913300	4423700
Q20953	Q20953	Protein RING1A	RING1A	3233300	3233300	3391000	4132700	2500000	913300	4423700
Q20953	Q20953	Protein RING1B	RING1B	3233300	3233300	3391000	4132700	2500000	913300	4423700
Q20953	Q20953	Protein RING1A	RING1A	3233300	3233300	3391000	4132700	2500000	913300	4423700
Q209										

Q9Y2W1	Thyroid hormone receptor-associated protein 3	THRAP3	31167	48083	85933	0	0	125530	0
Q9Y2X1	Nucleolar protein 58	NCP58	23260	59560	0	0	59940	369390	79650
Q9Y2Z0	Suppressor of G2 allele of SKP1 homolog	SLUG1	91010	0	484360	0	0	0	339280
Q9Y133	UR siRNA-associated 5m-like protein L5m2	LSM2	0	0	6688900	0	0	0	0
Q9Y1B3	Putative RNA-binding protein Luc7-like 2	LUC7L2	830640	1435200	782050	970330	1038700	1950900	1247600
Q9Y1A4	Ribosomal RNA-processing protein 7 homolog A	RBP7A	210450	0	0	0	535380	0	0
Q9Y1B4	Splicing factor 3B subunit 6	SF3B6	706490	3386500	3176000	4259600	15483000	3668200	1507200
Q9Y1B7	39S ribosomal protein L11, mitochondrial	MRPL11	955790	0	0	0	0	0	0
Q9Y1B9	RBP15-like protein	RBP15	271540	1019300	0	0	827970	0	0
Q9Y1C1	Nucleolar protein 16	NCP16	606960	1661500	0	0	3049500	0	0
Q9Y1C6	Peptidyl-prolyl cis-trans isomerase-like 1	PPI1	1415000	1878000	3731000	17819000	3701000	9662100	9260800
Q9Y1A4	Serine-threonine kinase receptor-associated protein	STRAP	1916000	1578000	5895400	29381000	11580000	16237000	22058000
Q9Y1D0	HR23-like splicing ligase Rb28 homolog	RT1CB	1035500	2276100	0	0	948210	0	0
Q9Y1H1	F box only protein 7	FBOX7	352870	1326600	2421800	2133300	0	725140	100280
Q9Y1F9	Nuclear complex protein 2 homolog	NCC2L	0	0	0	0	355800	0	0
Q9Y1U8	60S ribosomal protein L36	RPL36	45495000	412100000	0	41492000	387000000	8986600	44189000
M870D	Chromatin target of PRMT1 protein	CHTOP	1512600	2210400	0	0	2515400	0	0
Q9Y1G0	HBS1-like protein	HBS1L	566630	846570	0	38607	352390	184090	110690
Q9Y1G2	Talin-1	TN1	432070	21340	0	426870	23842	39431	294400
Q9Y1C2	TRPM8 channel-associated factor 1	TCAF1	0	0	126430	746590	510100	218580	469350
Q9Y1B3	Ubiquitin carboxyl-terminal hydrolase 15	USP15	679540	121430	98076	1540500	323480	411470	993050
Q9Y1A5	E3 ubiquitin-protein ligase RNF115	RNF115	0	0	0	1132600	789020	563470	516230
Q9Y1W2	Ribosomal biogenesis protein LAST1	LAST1	618830	879380	0	222040	738520	0	125310
Y555E	UR siRNA-associated 5m-like protein L5m4	LSM4	4601700	13341000	168290	23424200	2452000	4634700	10386000
Q9Y1B6	PAX3- and PAX7-binding protein 1	PAXBP1	0	0	660380	0	311820	706370	112570
Q9Y1B8	Nucleoside diphosphate kinase 7	NME7	145500	389650	0	39200	1176500	2020900	337230
Q9Y1B2	FACT complex subunit SP16	SUPT16H	1207100	1492500	0	0	214880	0	0
Q9Y1A9	Mitochondrial import inner membrane translocase subunit Tim8B	TIM8B	3304400	3077100	1880300	0	4932300	3113400	1317300
Q9Y1A1	Mitochondrial import inner membrane translocase subunit Tim13	TIM13	2105000	1803800	0	2462300	9647000	11169000	11447000
Q9Y1B4	Signal recognition particle receptor subunit beta	SRFBP2	2224400	52450	0	2399710	404170	0	65500
Q9Y1A3	Mannose-1-phosphate guanylyltransferase beta	GMPFB	423910	0	0	0	0	153560	0
Q9Y1C9	General transcription factor 3C, polypeptide 3	GTF3C3	0	0	0	0	0	81679	0
Q9Y1S9	RNA-binding protein 8A	RBMA8	1749000	2095100	3810600	21271000	9419900	5804400	8417300
Q9Y1T5	Ubiquitin carboxyl-terminal hydrolase 16	USP16	381400	529800	0	86584	937590	0	0
Q9Y1C0	Melanoma-associated antigen D1	MAGEE1	0	0	0	153540	109170	82745	50578
Q9Y1Z4	Heme-binding protein 2	HEBP2	2425800	0	0	2326900	355700	615000	1664400
Q9Y1G8	Leucine-rich repeat flightless-interacting protein 2	LRRIP2	9279300	6143100	8708900	13878000	10579000	10739000	10760000
Q9Y1T7	Phosphoserine aminotransferase	PSAT1	1025000	3604700	147150	11132000	1129600	2396600	7567200
Q9Y1E7	Spindlin-1	SPIN1	336980	1093900	0	0	0	77081	0
Q9Y1W6	28S ribosomal protein S18b, mitochondrial	MRP518B	724670	1254000	0	283500	1649300	0	448070
Q9Y1T8	Coatomer subunit gamma-1	COG1	231830	0	0	264070	0	0	0
Q9Y1E6	Chloride intracellular channel protein 4	CLIC4	2225900	1868600	0	344890	0	0	1958800
Q9Y1A4	Cilia- and flagella-associated protein 20	CFAP20	0	817470	220030	0	123430	2032400	514000
Q9Y1E3	Adrenalin	SCN	1394400	0	0	168320	415340	387750	519300
Q9Y1V7	Probable ATP-dependent RNA helicase DDX49	DDX49	0	866740	0	0	534340	0	0
Q9Y1B8	SIC23-interacting protein	SIC23IP	161840	0	0	0	0	0	88257
M870E	Apoptotic chromatin condensation inducer in the nucleus	ACIN1	374040	796600	44907	67117	61495	35087	0
M870A5	Histone deacetylase complex subunit SAP18	SAP18	169730	0	0	1215500	590750	0	0

Gene	Protein	UniProt	Ensembl	RefSeq	NCBI	KEGG	UniProt	Ensembl	RefSeq	NCBI	KEGG	UniProt	Ensembl	RefSeq	NCBI	KEGG
BRWV6C20WV6-2QBW6W	See family domain-containing protein 1	SCZ1	0.000170044	5.70166E-05	9.9848E-05	0.000130828	0.0001937	5.91807E-05	2.9198E-05	0.000109777	0.000109829	1.179759E-07	0.000663665	3.171935E-09	0.000170044	0.000170044
UBIQUITIN-LINKING COMPLEX 1	Ubiquitin-like domain-containing C20 phosphatase 1	UBCP1	0.000044632	0.00001574	6.80035E-05	0.000123045	0.000065468	0.000157347	0.000127255	0.000127255	0.000065468	0.000032633	0.000103359	0.00008371	1.4650551E-07	0.000044632
PE1 proteolytic signal-containing nuclear protein	PE1 proteolytic signal-containing nuclear protein	PEP1	0.000140622	0.000144442	0.000251361	0.000120893	0.000060999	0.000124164	0.000156182	0.000156182	0.000156182	0.000140622	0.000140622	0.000140622	2.5724403E-07	0.000140622
Probable RNA polymerase II subunit 1	Probable RNA polymerase II subunit 1	TRB1	0.000160308	0	0	0.000107772	0.000117161	0.000117161	0.000117161	0.000117161	0.000117161	0.000160308	0.000160308	0.000160308	0.000160308	0.000160308
ATXN2L	Ataxin-2-like protein	ATXN2L	6.21725E-05	3.65076E-05	0	6.68395E-05	6.63446E-05	0	0.000130694	1.80002E-05	0	1.28776E-05	4.43814E-05	3.87474E-05	1.1987761E-05	0.000130694
USP48	USP48 small nuclear ribonucleoprotein Psp1	PRP31	0.001603935	0.000091319	0.000022086	0.000175268	0.00124306	0.001205219	0.001826276	0.001804783	0.000470204	0.00004213	0.000140048	0.000139491	1.4861893E-07	0.001603935
AT18C	AT18C interaction protein	AT18C	0	0.000402627	0.000034654	0.000168705	0.000257501	0.000174417	0.000838868	0.001550815	0.000155249	0.000176627	0.000154489	1.051717029	0.000168705	1.573570E-05
PAR6A	Par6alpha component 1	PAR6A	0.000414715	0.40345E-05	0	0.000232507	0	0.000198111	0.000198111	0.000198111	0.000198111	0.000198111	0.000198111	0.000198111	0.000198111	0.000414715
DNAH9	DNAH9 homolog family C member 9	DNAH9	7.06844E-05	0.00021778	0.000119902	0.000106037	0	0	0	0	0	0.00018118	3.53476E-05	0.2589499E-04	0.000119902	0.000119902
ITIH2	ITIH2	ITIH2	2.29932E-05	2.55117E-06	1.80209E-06	1.30116E-06	6.02096E-06	0	2.29622E-06	0	0	1.67105E-05	2.59002E-06	8.82416E-07	0.1501054E-03	0.1996440E-06
TRXN	Histone H1X	TRXN	0.00155887	0.000171583	0	0.000094234	0.000197825	0	0.000124604	6.8139E-05	0	0.000144559	0.000170719	9.938E-05	1.2468921E-07	0.00155887
TCF7L1	Tcf7-like protein 1	TCF7L1	0.00013845	0	0.00003377	6.33816E-05	0.000156084	0	0.000156084	0	0	4.12438E-05	0.000156084	0.000156084	0.00013845	0.00013845
CELSR3	Cell surface-specific I-lectin-like transmembrane receptor family class 3 member 3	CELSR3	0	0	0	0	0	0	0	0	0	0	0	0	0	0
PCSK9	Protein converting enzyme 1	PCSK9	4.464E-05	0	0	0.20717E-05	9.9300E-05	5.85709E-05	0	1.488E-05	6.67917E-06	4.16313E-05	3.3356684E-05	0.162428E-05	0.0001464E-05	4.464E-05
AP3 complex subunit sigma-1	AP3 complex subunit sigma-1	AP3S1	6.84937E-05	0	0	0	9.53498E-05	0.000182049	0	0	0	2.31446E-05	0	0.24386E-05	0.000182049	0.000182049
Heat shock protein 105 kDa	Heat shock protein 105 kDa	HSP105	0.00115277	0.000591893	0.000169347	0.000069428	0.000066791	0.000336827	0.000130087	0.000130087	0.000116487	0.000178817	0.000150835	0.000191593	1.1891381E-07	0.00115277
UNC119B	UNC119B	UNC119B	0.00002559	0	0.000023967	9.70045E-05	5.00046E-05	0.00015641	0.000049526	1.63444E-06	0.000000000	9.42008E-05	0.000160161	0.6350468E-06	0.00002559	0.00002559
LRN4	Leu-1-related protein 4B	LRN4	0.00028735	2.15181E-05	0	0.000050515	0	0.85396E-05	0	0.85396E-05	0	0.000132081	0.816022E-05	2.84813E-05	0.00028735	0.00028735
PCSK2	Protein converting enzyme 2	PCSK2	0	0	0	7.94161E-05	0	0	0	0	0	1.44032E-06	2.47437E-05	0.1774789E-07	0.000132081	0.000132081
NUFIP3	Nucleolar protein complex protein NUFIP3	NUFIP3	0.000057399	0.000047335	0.000048478	0.000019718	0.000125601	0.000167966	4.81925E-05	4.99474E-05	7.64888E-06	0.00004317	0.000131945	4.70023E-05	0.000057399	0.000057399
MURF1	MURF1	MURF1	9.8191E-05	0	0	0.000102025	0	0	0	0	0	3.002E-05	0.30242E-05	1.3311E-05	0.000102025	0.000102025
ANKRD58	Ankyrin domain containing protein 58	ANKRD58	0.000094642	0.000087967	0.000144487	0.000069769	0.000179149	0.000048814	0.000033318	0.000033318	0.000033318	0.000094642	0.000094642	0.000094642	0.000094642	0.000094642
APC1	Adenomatous polyposis coli 1	APC1	0.00024255	0.000202383	1.16705E-05	0.000165481	1.78426E-06	0.000300215	0.000178047	0.000126452	0.000030979	0.000178047	0.000054844	0.000094642	0.00024255	0.00024255
HMC2	Histone deacetylase 2/histone deacetylase 1	HMC2/HDAC1	0.000102689	0.000027163	5.97007E-06	0.000103579	0.000022066	0.000103579	0.000124951	0.000046519	5.04961E-05	0.000124951	0.000013076	0.000139714	1.4500910E-07	0.000102689
SYMPK	Sympkin	SYMPK	1.582E-05	0	3.17596E-05	0	0	0.000187132	0	0	0	5.27334E-06	1.25318E-05	0.0544E-05	2.374673E-07	0.000187132
GGH	Guanine glyoxylase	GGH	0	4.40171E-05	0	0.000103735	0	0	0	0	0	1.47408E-05	5.12107E-05	0	0	0.000103735
COX2A2	Cytochrome c oxidase subunit 2A2	COX2A2	0	0	0	1.82036E-05	1.37006E-05	0	0	0	0	0	0	0	0	0
RNA52	RNA52	RNA52	0.0000466	0.0000186	0.58333E-06	1.20093E-05	5.28248E-05	0.00018407	4.00000E-05	0	0	6.67516E-06	0.000022775	1.35446E-05	0.0000466	0.0000466
UPP1	Uridylate phosphorylase 1	UPP1	0.000007299	1.8033E-05	3.25920E-05	0.00002486	5.911E-05	4.63474E-05	0.0001841	0.00011841	7.99274E-05	0.00001479	0.00011352	4.8488E-05	0.000007299	0.000007299
CPDPO	CPDPO	CPDPO	0.000039632	0.000150909	0	0.000078913	0.000179973	0.000129607	0.00018202	0.00018202	0.00018202	0.000039632	0.000039632	0.000039632	0.000039632	0.000039632
GRW4	GRW4	GRW4	0	0	4.19409E-06	0	0	0	0	0	0	0	0	0	0	0
KHSP8	Heat shock protein 8 kDa	KHSP8	0.00009923	0.00007911	0.000028132	0.00004011	0.000107144	0.00003136	0.00017613	0.000132545	0.00010903	0.00018279	0.000176325	1.4644323E-06	0.00009923	0.00009923
TRAF3IP1	TRAF3IP1	TRAF3IP1	5.17025E-05	1.49548E-05	0	0.00013056	0	0	0.86746E-05	0	0	2.22477E-05	4.51397E-05	1.22495E-05	2.0324047E-07	0.00013056
USP7	USP7	USP7	0	0	5.48871E-05	0	0	0	0	0	0	0	0	0	0	0
USP9	USP9	USP9	8.19590E-06	4.8212E-06	0.36058E-05	0	2.9707E-05	4.19368E-05	0.00003747	3.05959E-05	4.27394E-06	1.99907E-05	0.000136543	4.6510485E-06	8.22642E-06	3.194201E-07
USP10	USP10	USP10	0.000109425	0	3.20312E-05	0.00008713	1.61676E-05	0.0001818	0.000032419	0.00017882	5.84017E-05	6.00349E-05	0.000136543	2.7184264E-07	0.000109425	0.000109425
USP9B	USP9B	USP9B	0.000044632	0.00014637	8.4827E-05	0.00000816	0.000102462	0.000003263	0.000003263	0.000003263	0.000003263	0.000044632	0.000044632	0.000044632	0.000044632	0.000044632
USP9C	USP9C	USP9C	0.000044632	0.00014637	8.4827E-05	0.00000816	0.000102462	0.000003263	0.000003263	0.000003263	0.000003263	0.000044632	0.000044632	0.000044632	0.000044632	0.000044632
USP9D	USP9D	USP9D	0.000044632	0.00014637	8.4827E-05	0.00000816	0.000102462	0.000003263	0.000003263	0.000003263	0.000003263	0.000044632	0.000044632	0.000044632	0.000044632	0.000044632
USP9E	USP9E	USP9E	0.000044632	0.00014637	8.4827E-05	0.00000816	0.000102462	0.000003263	0.000003263	0.000003263	0.000003263	0.000044632	0.000044632	0.000044632	0.000044632	0.000044632
USP9F	USP9F	USP9F	0.000044632	0.00014637	8.4827E-05	0.00000816	0.000102462	0.000003263	0.000003263	0.000003263	0.000003263	0.000044632	0.000044632	0.000044632	0.000044632	0.000044632
USP9G	USP9G	USP9G	0.000044632	0.00014637	8.4827E-05	0.00000816	0.000102462	0.000003263	0.000003263	0.000003263	0.000003263	0.000044632	0.000044632	0.000044632	0.000044632	0.000044632
USP9H	USP9H	USP9H	0.000044632	0.00014637	8.4827E-05	0.00000816	0.000102462	0.000003263	0.000003263	0.000003263	0.000003263	0.000044632	0.000044632	0.000044632	0.000044632	0.000044632
USP9I	USP9I	USP9I	0.000044632	0.00014637	8.4827E-05	0.00000816	0.000102462	0.000003263	0.000003263	0.000003263	0.000003263	0.000044632	0.000044632	0.000044632	0.000044632	0.000044632
USP9J	USP9J	USP9J	0.000044632	0.00014637	8.4827E-05	0.00000816	0.000102462	0.000003263	0.000003263	0.000003263	0.000003263	0.000044632	0.000044632	0.000044632	0.000044632	0.000044632
USP9K	USP9K	USP9K	0.000044632	0.00014637	8.4827E-05	0.00000816	0.000102462	0.000003263	0.000003263	0.000003263	0.000003263	0.000044632	0.000044632	0.000044632	0.000044632	0.000044632
USP9L	USP9L	USP9L	0.000044632	0.00014637	8.4827E-05	0.00000816	0.000102462	0.000003263	0.000003263	0.000003263	0.000003263	0.000044632	0.000044632	0.000044632	0.000044632	0.000044632
USP9M	USP9M	USP9M	0.000044632	0.00014637	8.4827E-05	0.00000816	0.000102462	0.000003263	0.000003263	0.000003263	0.000003263	0.000044632	0.000044632	0.000044632	0.000044632	0.000044632
USP9N	USP9N	USP9N	0.000044632	0.00014637	8.4827E-05	0.00000816	0.000102462	0.000003263	0.000003263	0.000003263	0.000003263	0.000044632	0.000044632	0.000044632	0.000044632</	

Q99576,Q5JRJ0,E7EWD5,Q99576-4,Q99576-3,Q5JRJ2,D6R092,D6R091,H0Y865,H7BZ77,Q15714-3,Q99508-2,Q99508,Q15714-3,Q75157-2,Q75157,Q15714	TSC22 domain family protein 3	TSC2D3	0	0	0	0.003396272	0.001859966	0.001543727	#DIV/0!	0.01665358
3QRMS,Q8N138-4,Q8N138,JKT9,F6W514,F8VXD5,Q8P053,Q33FV1	ORM1-like protein 3,ORM1-like protein 1,ORM1-like protein 2	ORMDL3,ORMDL1,ORMDL2	0	0	0	0.000671664	0.001530214	0.000841951	#DIV/0!	0.01805544
Q7L5D6,Q7L5D6-2,C9JPA8,C9JHN8,C9IY46	Golgi to ER traffic protein 4 homolog	GET4	0	0	0	0.003746692	0.001479127	0.002169422	#DIV/0!	0.021328523
Q3R909,Q9LNF1-2,Q9LNF1,Q5H907,ADA087K070,G5E9N2,Q12816-5,Q12816-2,Q12816-3,Q12816-4,Q12816	Melanoma-associated antigen D2	MAGED2	0	0	0	0.000652072	0.000469927	0.000226067	#DIV/0!	0.021940047
P51991-2	Heterogeneous nuclear ribonucleoprotein A3	HNRNPA3	0	0	0	0.000182671	6.87591E-05	0.000210234	#DIV/0!	0.023716433
Q00767	Acyl-CoA desaturase	SCD	0	0	0	0.000257698	8.73424E-05	0.000165572	#DIV/0!	0.025884047
Q6ZVM7-3,Q6ZVM7,87ZZU2,Q6ZVM7-2,Q6ZVM7-5,F5H356,Q6ZVM7-4,K7ENB0	TOM1-like protein 2	TOM1L2	0	0	0	0.000277559	0.000332095	0.000677326	#DIV/0!	0.026595249
ADA087WWL9,A2AEA2,P10321,F6UDH7,Q31612,P30499,Q956	HLA class I histocompatibility antigen, Cw-7 alpha chain	HLA-C	0	0	0	0.001834072	0.000531729	0.001059821	#DIV/0!	0.039188405
04FW928,Q09160	mRNA cap guanine-N7 methyltransferase	RNMT	0	0	0	0.000179189	7.39906E-05	0.000287044	#DIV/0!	0.042907374
K7EP06,Q43148,Q43148-2,K7ERH6	Protein yyppee-like 5	YPEL5	0	0	0	5.64568E-05	9.66227E-05	0.000190842	#DIV/0!	0.045079463
626599										
Decreased DAPs (Fold change = 0)										
ADA087WVM7,V9GYPS,ADA087WWQ2,Q92979	Ribosomal RNA small subunit methyltransferase NEP1	EMG1	7.77146E-05	6.25182E-05	9.72227E-05	0	0	0	0	0.001401875
QBYS1	Peptidase M20 domain-containing protein 2	PM20D2	5.63666E-05	7.25825E-05	2.76166E-05	0	0	0	0	0.016546213
P35658-2,P35658-4,P35658,P35658-3,P35658-5,H0YF36,H0Y837,H0YD54,EPKXZ2,B7ZAV2	Nuclear pore complex protein Nup214	NUP214	0.000175602	5.56479E-05	0.000256509	0	0	0	0	0.049488264

Table S4. DAPs (MG132 12 h / DMSO)

Protein IDs	Protein names	Gene names	DMSO #1	DMSO #2	DMSO #3	MG132 12 h #1	MG132 12 h #2	MG132 12 h #3	Fold-change	p-value
Q504T8;K7END3;K7EN9	Midolin	MDIN	0	0	2.6197E-06	0.001307119	0.00080678	0.00041946	999.981413	0.02591987
Q5VYK3;J3K1N16;R4GM1;F6XAC5	Proteasome-associated protein ECM29 homolog	ECM29;AAO368	4.42319E-05	1.31092E-05	0	0.00598357	0.007158973	0.004043109	299.7089309	0.002375018
Q9NR09	Baculoviral IAP repeat-containing protein 6	BIRC6	2.71608E-06	0	0	0.00023504	0.000325905	0.000119613	250.5677305	0.019355629
Q95071-2	E3 ubiquitin-protein ligase UBR5	UBR5	2.32211E-06	0	0	0.000161362	0.0002129E-05	6.10429E-05	188.6336578	0.032679184
2:Q95071;E7EMW7;E7ETB4;E5RFK7	Ubiquitin-like protein 4A	UBL4A	0.000109133	0	0	0.003744665	0.005317357	0.003303148	113.3039492	0.002622913
P11441;Q5HYH1;F9W870										
P46379-2;P46379;P46379-3;P46379-5;P46379-6										
4:X6REW1;F656P2;F6UR09;F6U1F2;F6X7	Large proline-rich protein BAG6	BAG6	0	0.000105502	0	0.004715918	0.003614143	0.002353736	101.2850735	0.006671895
U0;H0Y71;F6R6G75;F6WML8;F6VEM6;F6X9W3;F6U341;H0Y4L1;F6T;C96;H0Y7K4										
K7EKW3;H0Y759;H0Y583;E7ESS3;O9S1										
64;Q17RG4-2;Q17RG4										
Q9P0P0;C911C6;F9WBU5;C9J391;H7C4	E3 ubiquitin-protein ligase RNF181	RNF181	0.000551718	0.001387169	0	0.034181961	0.03836681	0.040000681	57.89574107	3.21157E-05
26										
Q5T457-3;Q5T457-4;Q5T457;Q5T457-2;Q5T457-5;X6RE05;X6R960	E3 ubiquitin-protein ligase UBR4	UBR4	5.90453E-06	0	0	0.000117508	0.000126661	7.88999E-05	54.70522566	0.002026093
Q5TDH0;Q5TDH0-3;Q5TDH0-2	Protein DD11 homolog 2	DD12	2.0655E-06	0	0	0.00017058	0.00032434	0.000472766	47.3341328	0.002197353
2:HOY14;H0Y90;Q8WU10										
B7AJY7;O758B2;B7A1Y5;O758B2-2;B7A1	26S proteasome non-ATPase regulatory subunit 10	PSMD10	0.000119373	0.000343228	0	0.00449333	0.004314899	0.00204458	24.3377729	0.004874027
Q9LHD9	Ubiquitin-2	UBLQ2	0.000134753	0	0	0.000649798	0.000562198	0.001109737	17.22947919	0.014256502
Q13501;E7EMC7;Q13501-2;E9PW8;E3W990;C9JR8;D6R8F1;C9J6	Sequestosome-1	SQSTM1	0.000168414	0.000102116	0.000128113	0.003080351	0.00172569	0.001735708	16.55955077	0.010413812
J8										
Q8TAT6;Q8TAT6-2;J3L49	Nuclear protein localization protein 4 homolog	NPLOC4	1.63884E-05	0	0	0.000121403	9.69641E-05	4.22108E-05	15.90011672	0.027639663
Q8WVY7	Ubiquitin-like domain-containing CTD phosphatase 1	UBLCP1	0.000944527	0.00087154	6.86303E-05	0.010322725	0.009722655	0.006065749	14.14079798	0.002237041
Q15294;Q15294-3;O15294-2;O15294-4;C9JZL3;H7C17	UDP-N-acetylglucosamine--peptide N-acetylglucosaminyltransferase 110 kDa subunit	OGT	3.29908E-05	1.00179E-05	1.91412E-05	0.000248711	0.000224067	0.000290949	12.28847725	0.000345839
Q9GZL8;H3BU14;H3BM09;H3BP64;H3B8										
T8;H3BSV6;H3BT12;H3BQQ6;Q6P4H7;H3BSF0;H3BU93;H3BN22;H3BNK9;H3B8	Protein FAM192A	FAM192A;NIP30	0.00850783	0.007910531	0.005092945	0.064974116	0.116111521	0.079868141	12.13100582	0.00632485
PH9;H3BP9										
Q7Z6Z7-2;Q7Z6Z7										
3:Q7Z6Z7;Q7Z6Z7;AD087146;Q5H96	E3 ubiquitin-protein ligase HUWE1	HUWE1	2.7482E-05	1.96869E-05	1.36745E-05	0.000305139	0.000231806	0.00194483	12.02070183	0.002408927
3:AD087X153										
Q06323;Q06323-3;Q06323-2;H0YKK6;H0YU12	Proteasome activator complex subunit 1	PSME1	0.025208147	0.028094984	0.023623931	0.309624972	0.345869905	0.211713255	11.27078175	0.002767243
2:H0YKK6;H0YU12										
AD087X12;Q9JUL4;H0YM70;H0YGL1;H0YLD2;H0YKU2	Proteasome activator complex subunit 2	PSME2	0.026252794	0.03063095	0.024590289	0.303265537	0.311526922	0.302804341	11.22127261	1.24829E-07
Q981Y7;E9PIX0	Protein HGH1 homolog	HGH1	4.05135E-05	0	0	0.000183833	9.49139E-05	0.000161376	10.86361679	0.01126131
P54578										
2:P54578;A6N1A2;B7Z4N8;J3QQ7E;J3K5	Ubiquitin carboxyl-terminal hydrolase 14;Ubiquitin carboxyl-terminal hydrolase	USP14	0.001341434	0.000355867	0.000798707	0.009509058	0.006948791	0.0096251	10.44986497	0.001023673
55;H0Y4A7										
Q9H7D7-										
2:Q9H7D7;H0Y9R3;C9JCS7;H0Y917;Q9	WD repeat-containing protein 26	WDR26	3.28769E-05	0	0	6.36483E-05	9.42701E-05	0.0001712	10.01062547	0.043243042
H7D7-3;Q9H7D7-4										
AD087X153										
5:Q8TCT9;Q8TCT9-4;Q8TCT9-2	Minor histocompatibility antigen H13	HM13	4.26143E-05	0	0	0.000115051	0.000144898	0.000129587	9.98573945	0.001206636
P54725-2;P54725-3;P54725;K7EN0;K7ELW1;K7EQ16	UV excision repair protein RAD23 homolog A	RAD23A	0.000753452	0.000423776	0	0.005142909	0.003570177	0.002993219	9.943961055	0.006635184
Q13617;Q13617-2;Q13617-3;Q13617-4	Cullin-2	CUL2	0	1.32032E-05	0	6.11925E-05	4.10539E-05	2.47963E-05	9.622092364	0.029218529
Q9H9L7;B4DQ;P0H0YEQ5;Q9H9L7-2	Akirin-1	AKIRIN1	0.001066905	0.000577518	0	0.005223821	0.006077332	0.002561854	8.43031709	0.020949677
Q86YQD;Q96MX6										
2:Q96MX6;Q8ND98;H7C389;F6U119;D13	WD repeat-containing protein 92	HZGU;WDR92;K2FZ;K4348156	7.59424E-05	1.11023E-05	8.06744E-06	0.000260126	0.000151569	0.000372679	8.246839581	0.027261199
Q43396;K7ER66;K7EM9;K7EP87;K7EKG	Thioredoxin-like protein 1	TXN1L	0.023496098	0.016486823	0.014997885	0.14023405	0.182225753	0.119387174	8.036389342	0.002301785
2;K7EM7										
F5GWN1;J3KRPE;J3Q572;K6R312;J3QQ	Protein SSKT	SS18	0.000382923	0.000175425	0	0.000822752	0.0002026305	0.001244257	7.653489934	0.043256142
M2J3K7;J3Q5QW2;Q15532-2;Q15532-1										
Q6KCM8;Q95579-3;Q95579-2	Tumor necrosis factor alpha-induced protein 8	TNFAIP8	0	0	0.000162659	0.000477753	0.000178848	0.000515363	7.222808418	0.04789648
Q95379;Q95379-4										
P54727;Q5W055;P54727-2	UV excision repair protein RAD23 homolog B	RAD23B	0.013665458	0.005421185	0.004634043	0.052797502	0.043828662	0.054891849	6.387688569	0.000668588
2:Q5W055;H0Y579										
Q98XR0-2;Q98XR0;K7EP6;K7EJ21	Queuine tRNA-ribosyltransferase	QTRT1	0	0	5.64023E-05	0.000105274	9.88551E-05	0.000137844	6.063095271	0.013046327
P52657;H0YK39;A8MYR4;REV_Q6LUB99	Transcription initiation factor IIA subunit 2	GTF2A2	0.0001126	0	0.000789633	0.001898924	0.001932597	0.001548378	5.963871281	0.005626109
P46821;D6RA32;D6RA40;D6RC12;D6RG	Microtubule-associated protein 18;MAP1B heavy chain;MAP1 light chain L1	MAP1B	2.86172E-05	5.59474E-06	1.32401E-05	0.000146261	6.16487E-05	7.39825E-05	5.93672685	0.045813669
Q35H80	Akirin-2	AKIRIN2	0.012132132	0.017596427	0.018242226	0.050341738	0.04662083	0.016198308	5.915350675	0.038812213
P51571;A6NLM8	Transacon-associated protein subunit delta	SSRA	0.000319812	0.000096042	6.77865E-05	0.002602889	0.003277672	0.00181957	5.712335975	0.013146955
P15104;AD087WJ1	Glutamine synthetase	GLUL	0.000256008	0.000120041	0	0.000738291	0.000818367	0.000325509	5.034177518	
Q15370;88ZU8;Q15370-2;J3L0M9	Transcription elongation factor B polypeptide 2	TCEB2	0.006020543	0.001866655	0.00489331	0.026495562	0.020065761	0.002179371	4.995560250	0.001607258
C9JY29;P30876;C9J4M6	DNA-directed RNA polymerase;DNA-directed RNA polymerase II subunit RP2B	POLR2B	0.000103062	5.80022E-05	6.47012E-05	0.000130687	0.00044847	0.00021668	4.867690905	0.017473961
Q05086-3;Q05086;Q05086-2;S4R306	Ubiquitin-protein ligase E3A	UBE3A	0.001593022	0.001644789	0.001400348	0.007506784	0.007054642	0.007206878	4.585529931	0.000815833
Q43765;K7EMD6	Small glutamine-rich tetrapeptide repeat-containing protein alpha	SGTA	0.00060897	0.000484976	0	0.002035314	0.001584418	0.00103544	4.25585291	0.02597105
Q52525;ZAS;Q5JUP7	Transitional endoplasmic reticulum ATPase	VCP	0.00240812	0.001666652	0.000233873	0.011279763	0.00763289	0.007198973	4.246751138	0.019110354
Q9NSE4	isoleucine--tRNA ligase, mitochondrial	IARS2	2.35408E-05	1.82328E-05	0	6.66065E-05	4.87434E-05	6.15416E-05	4.234904401	0.007173903
Q95163;F5H210	Elongator complex protein 1	IKKAP	3.63375E-05	1.04038E-05	0	9.38102E-05	5.1406E-05	5.15588E-05	4.209600921	0.048115753
Q5JV3-3;Q5JV3-2;Q5JV3;Q5JV3-4	PCI domain-containing protein 2	PCD2	8.3682E-05	1.41319E-05	0.0001109	0.000334006	0.00035953	0.000170322	4.186863742	0.029874651
F8VUX1;F8VY3;F8W016;F5H4R6;P5520										
9-										
2:P5209;F8V959;B7Z9C2;H0YIV4;83KV	Nucleosome assembly protein 1-like 1	NAP1L1	0.00647786	0.000879342	0	0.012739026	0.007896068	0.009730652	4.127349719	0.03610953
44;F8W020;F8V816;H0YHC3;F8W118;B7										
VR12;F8V85;H0YH88;B7Z4K9										
P61289;P61289-2;P61289-3;K9J957;K7E5G5;AD087WTV2;K7ENH	Proteasome activator complex subunit 3	PSME3	0.137137905	0.151226547	0.098674635	0.419495561	0.552215565	0.589557436	4.03387826	0.001914971
2;B728D3;K7EJF8										
B5MD17;J3K505;P83916;K7EL4A;C9JWS	Chromobox protein homolog 1	CBX1	0.000227722	0	0.000435851	0.001020718	0.000524042	0.001112743	4.004837619	0.040167109
Q9JUL1;P52434;P52434-4;P52434-3;P52434-2;P52434-5	DNA-directed RNA polymerases I, II, and III subunit RPABC3	POLR2H	0.001959362	0.001091095	0.001180136	0.00458731	0.005251185	0.006730431	3.916454858	0.003995427
Q9Y4E8-2;Q9Y4E8-3;Q9Y4E8;Q9Y4E8-4;F8W0H4;H0Y31;F8VZG8;F8VY7;H0Y	Ubiquitin carboxyl-terminal hydrolase 15	USP15	0.000145973	1.81834E-05	2.31162E-05	0.00028193	0.000180155	0.000626361	3.868405223	0.02645132
HML4;H0Y126;H7C189;Q13107-2;Q9HY6;Q9HY6-3;Q9HY6-6										
2:Q9HY6-4;Q9HY6-5										
5:41;Q9JG22;C9J583;F8W054;F8W	DNA-directed RNA polymerase I subunit RPA2	POLR1B	0.000442899	0.000124741	0.000129857	0.001071451	0.000752685	0.0		

H0Y7A7:P62158:E7ETZ0:E7EMB3:Q96H Y3:G3V361:MQQZ52:F8WBRS:G3V226G 3V479Y27462:C37719:P02585 Q1571:Q15717	Calmodulin	CALM2;CALM1	0.028995277	0.008539006	0.017065185	0.037676811	0.048606544	0.038094586	2.278006472	0.028358378
2:MQQZ95:MDR055:81AM48:81APV9:8 1:APY8:81AM49:Q12926- 2:Q12926:P26378-4:P26378-2:P26378- 5:P26378:P26378-3	ELAV-like protein 1	ELAVL1	0.002483437	0.002528279	0.002248316	0.00455097	0.004444328	0.006046559	2.017872014	0.007783566
P31946-2:P31946:Q4VY20:Q4V19 P83876:K75L1:K7EP6A:K7EJUZ:K7EMX 5:K75L1:K75E07	14-3-3 protein beta/alpha:14-3-3 protein beta/alpha, N-terminally processed	YWHA8	0.004656257	0.006883846	0.001699	0.007598389	0.006075089	0.006653039	2.012078277	0.025913768
P08107:P08107-2:V9GZ37	Thioredoxin-like protein 4A	TXN14A	0.002203233	0.001266805	0.003592968	0.00543897	0.004458236	0.00410972	1.982678982	0.014879982
A0A087X211:P62333:H0VJCD:H0VJ58:H0 Y1T1:H0VJX2:H0VJ9:H0VJ1D2:H0VJY8 Q13200:Q13200-	Heat shock 70 kDa protein 1A	HSPA1A	0.467129414	0.370017624	0.534019157	0.81261502	0.830902955	1.040666741	1.957593222	0.007415828
2:Q12926:P26378-4:P26378-2:P26378- 5:P26378:P26378-3	26S protease regulatory subunit 10B	PSMC6	0.194707428	0.203247641	0.185465417	0.34528323	0.37695924	0.365847392	1.865018266	9.2297E-05
2:Q12926:P26378-4:P26378-2:P26378- 5:P26378:P26378-3	26S proteasome non-ATPase regulatory subunit 2	PSMD2	0.137767304	0.120892889	0.10190133	0.213486787	0.22290505	0.22713965	1.840272591	0.000814307
1:Z15:P11215-2 Q43242:H0VJG8:F5H8K4 Q9UNM6:13KNQ3:Q9UNM6- 2:A0A087WUL9:E9P138:H0YD73:E9PQG 3:E9PPD2:F8WB8 P10599:P10599-2 P43686:P43686-2 P17066:P48741 P02785:P02787 P40227:P40227-2:J3KR16 P62195:J3QJMT:J3QSE0:J3QRW1:J3KT Q9	26S proteasome non-ATPase regulatory subunit 3	PSMD3	0.192703235	0.176548271	0.125440409	0.327936737	0.313927079	0.256438185	1.815881706	0.010731784
2:Q12926:P26378-4:P26378-2:P26378- 5:P26378:P26378-3	26S proteasome non-ATPase regulatory subunit 13	PSMD13	0.234423954	0.163924845	0.187492413	0.338157256	0.365653827	0.357922406	1.812322298	0.002056608
1:Z15:P11215-2 Q43242:H0VJG8:F5H8K4 Q9UNM6:13KNQ3:Q9UNM6- 2:A0A087WUL9:E9P138:H0YD73:E9PQG 3:E9PPD2:F8WB8 P10599:P10599-2 P43686:P43686-2 P17066:P48741 P02785:P02787 P40227:P40227-2:J3KR16 P62195:J3QJMT:J3QSE0:J3QRW1:J3KT Q9	Thioredoxin	TXN	0.010303226	0.007898252	0.010909952	0.018689351	0.015719683	0.017505678	1.789493409	0.004089853
1:Z15:P11215-2 Q43242:H0VJG8:F5H8K4 Q9UNM6:13KNQ3:Q9UNM6- 2:A0A087WUL9:E9P138:H0YD73:E9PQG 3:E9PPD2:F8WB8 P10599:P10599-2 P43686:P43686-2 P17066:P48741 P02785:P02787 P40227:P40227-2:J3KR16 P62195:J3QJMT:J3QSE0:J3QRW1:J3KT Q9	26S protease regulatory subunit 6B	PSMC4	0.239815726	0.215152296	0.185328712	0.374695615	0.407262912	0.285617161	1.769471293	0.043301389
1:Z15:P11215-2 Q43242:H0VJG8:F5H8K4 Q9UNM6:13KNQ3:Q9UNM6- 2:A0A087WUL9:E9P138:H0YD73:E9PQG 3:E9PPD2:F8WB8 P10599:P10599-2 P43686:P43686-2 P17066:P48741 P02785:P02787 P40227:P40227-2:J3KR16 P62195:J3QJMT:J3QSE0:J3QRW1:J3KT Q9	Heat shock 70 kDa protein 6	HSPA6	0.02354706	0.031447754	0.047719256	0.055812556	0.067389213	0.070173697	1.748768923	0.016511504
1:Z15:P11215-2 Q43242:H0VJG8:F5H8K4 Q9UNM6:13KNQ3:Q9UNM6- 2:A0A087WUL9:E9P138:H0YD73:E9PQG 3:E9PPD2:F8WB8 P10599:P10599-2 P43686:P43686-2 P17066:P48741 P02785:P02787 P40227:P40227-2:J3KR16 P62195:J3QJMT:J3QSE0:J3QRW1:J3KT Q9	T-complex protein 1 subunit delta	CTC4	0.005575232	0.004673363	0.003238244	0.00849115	0.007180554	0.007294403	1.734917661	0.014895445
1:Z15:P11215-2 Q43242:H0VJG8:F5H8K4 Q9UNM6:13KNQ3:Q9UNM6- 2:A0A087WUL9:E9P138:H0YD73:E9PQG 3:E9PPD2:F8WB8 P10599:P10599-2 P43686:P43686-2 P17066:P48741 P02785:P02787 P40227:P40227-2:J3KR16 P62195:J3QJMT:J3QSE0:J3QRW1:J3KT Q9	T-complex protein 1 subunit zeta	CTC6A	0.010979883	0.00777022	0.005994958	0.015238795	0.013504136	0.01416762	1.724105636	0.017214999
1:Z15:P11215-2 Q43242:H0VJG8:F5H8K4 Q9UNM6:13KNQ3:Q9UNM6- 2:A0A087WUL9:E9P138:H0YD73:E9PQG 3:E9PPD2:F8WB8 P10599:P10599-2 P43686:P43686-2 P17066:P48741 P02785:P02787 P40227:P40227-2:J3KR16 P62195:J3QJMT:J3QSE0:J3QRW1:J3KT Q9	26S protease regulatory subunit 8	PSMC5	0.25575475	0.227850594	0.251653906	0.419041315	0.459439402	0.384446856	1.690446162	0.004264249
1:Z15:P11215-2 Q43242:H0VJG8:F5H8K4 Q9UNM6:13KNQ3:Q9UNM6- 2:A0A087WUL9:E9P138:H0YD73:E9PQG 3:E9PPD2:F8WB8 P10599:P10599-2 P43686:P43686-2 P17066:P48741 P02785:P02787 P40227:P40227-2:J3KR16 P62195:J3QJMT:J3QSE0:J3QRW1:J3KT Q9	26S proteasome non-ATPase regulatory subunit 11	PSMD11	0.176558215	0.169195837	0.192050797	0.324160822	0.306906059	0.273815082	1.68317239	0.001658485
1:Z15:P11215-2 Q43242:H0VJG8:F5H8K4 Q9UNM6:13KNQ3:Q9UNM6- 2:A0A087WUL9:E9P138:H0YD73:E9PQG 3:E9PPD2:F8WB8 P10599:P10599-2 P43686:P43686-2 P17066:P48741 P02785:P02787 P40227:P40227-2:J3KR16 P62195:J3QJMT:J3QSE0:J3QRW1:J3KT Q9	26S proteasome non-ATPase regulatory subunit 12	PSMD12	0.153654773	0.138221274	0.172209806	0.230342128	0.232389035	0.290505374	1.623054295	0.011927968
1:Z15:P11215-2 Q43242:H0VJG8:F5H8K4 Q9UNM6:13KNQ3:Q9UNM6- 2:A0A087WUL9:E9P138:H0YD73:E9PQG 3:E9PPD2:F8WB8 P10599:P10599-2 P43686:P43686-2 P17066:P48741 P02785:P02787 P40227:P40227-2:J3KR16 P62195:J3QJMT:J3QSE0:J3QRW1:J3KT Q9	Thioredoxin	TXN	0.010303226	0.007898252	0.010909952	0.018689351	0.015719683	0.017505678	1.789493409	0.004089853
1:Z15:P11215-2 Q43242:H0VJG8:F5H8K4 Q9UNM6:13KNQ3:Q9UNM6- 2:A0A087WUL9:E9P138:H0YD73:E9PQG 3:E9PPD2:F8WB8 P10599:P10599-2 P43686:P43686-2 P17066:P48741 P02785:P02787 P40227:P40227-2:J3KR16 P62195:J3QJMT:J3QSE0:J3QRW1:J3KT Q9	26S protease regulatory subunit 6B	PSMC4	0.239815726	0.215152296	0.185328712	0.374695615	0.407262912	0.285617161	1.769471293	0.043301389
1:Z15:P11215-2 Q43242:H0VJG8:F5H8K4 Q9UNM6:13KNQ3:Q9UNM6- 2:A0A087WUL9:E9P138:H0YD73:E9PQG 3:E9PPD2:F8WB8 P10599:P10599-2 P43686:P43686-2 P17066:P48741 P02785:P02787 P40227:P40227-2:J3KR16 P62195:J3QJMT:J3QSE0:J3QRW1:J3KT Q9	Heat shock 70 kDa protein 6	HSPA6	0.02354706	0.031447754	0.047719256	0.055812556	0.067389213	0.070173697	1.748768923	0.016511504
1:Z15:P11215-2 Q43242:H0VJG8:F5H8K4 Q9UNM6:13KNQ3:Q9UNM6- 2:A0A087WUL9:E9P138:H0YD73:E9PQG 3:E9PPD2:F8WB8 P10599:P10599-2 P43686:P43686-2 P17066:P48741 P02785:P02787 P40227:P40227-2:J3KR16 P62195:J3QJMT:J3QSE0:J3QRW1:J3KT Q9	T-complex protein 1 subunit delta	CTC4	0.005575232	0.004673363	0.003238244	0.00849115	0.007180554	0.007294403	1.734917661	0.014895445
1:Z15:P11215-2 Q43242:H0VJG8:F5H8K4 Q9UNM6:13KNQ3:Q9UNM6- 2:A0A087WUL9:E9P138:H0YD73:E9PQG 3:E9PPD2:F8WB8 P10599:P10599-2 P43686:P43686-2 P17066:P48741 P02785:P02787 P40227:P40227-2:J3KR16 P62195:J3QJMT:J3QSE0:J3QRW1:J3KT Q9	T-complex protein 1 subunit zeta	CTC6A	0.010979883	0.00777022	0.005994958	0.015238795	0.013504136	0.01416762	1.724105636	0.017214999
1:Z15:P11215-2 Q43242:H0VJG8:F5H8K4 Q9UNM6:13KNQ3:Q9UNM6- 2:A0A087WUL9:E9P138:H0YD73:E9PQG 3:E9PPD2:F8WB8 P10599:P10599-2 P43686:P43686-2 P17066:P48741 P02785:P02787 P40227:P40227-2:J3KR16 P62195:J3QJMT:J3QSE0:J3QRW1:J3KT Q9	26S protease regulatory subunit 8	PSMC5	0.25575475	0.227850594	0.251653906	0.419041315	0.459439402	0.384446856	1.690446162	0.004264249
1:Z15:P11215-2 Q43242:H0VJG8:F5H8K4 Q9UNM6:13KNQ3:Q9UNM6- 2:A0A087WUL9:E9P138:H0YD73:E9PQG 3:E9PPD2:F8WB8 P10599:P10599-2 P43686:P43686-2 P17066:P48741 P02785:P02787 P40227:P40227-2:J3KR16 P62195:J3QJMT:J3QSE0:J3QRW1:J3KT Q9	26S proteasome non-ATPase regulatory subunit 11	PSMD11	0.176558215	0.169195837	0.192050797	0.324160822	0.306906059	0.273815082	1.68317239	0.001658485
1:Z15:P11215-2 Q43242:H0VJG8:F5H8K4 Q9UNM6:13KNQ3:Q9UNM6- 2:A0A087WUL9:E9P138:H0YD73:E9PQG 3:E9PPD2:F8WB8 P10599:P10599-2 P43686:P43686-2 P17066:P48741 P02785:P02787 P40227:P40227-2:J3KR16 P62195:J3QJMT:J3QSE0:J3QRW1:J3KT Q9	26S proteasome non-ATPase regulatory subunit 12	PSMD12	0.153654773	0.138221274	0.172209806	0.230342128	0.232389035	0.290505374	1.623054295	0.011927968
1:Z15:P11215-2 Q43242:H0VJG8:F5H8K4 Q9UNM6:13KNQ3:Q9UNM6- 2:A0A087WUL9:E9P138:H0YD73:E9PQG 3:E9PPD2:F8WB8 P10599:P10599-2 P43686:P43686-2 P17066:P48741 P02785:P02787 P40227:P40227-2:J3KR16 P62195:J3QJMT:J3QSE0:J3QRW1:J3KT Q9	Thioredoxin	TXN	0.010303226	0.007898252	0.010909952	0.018689351	0.015719683	0.017505678	1.789493409	0.004089853
1:Z15:P11215-2 Q43242:H0VJG8:F5H8K4 Q9UNM6:13KNQ3:Q9UNM6- 2:A0A087WUL9:E9P138:H0YD73:E9PQG 3:E9PPD2:F8WB8 P10599:P10599-2 P43686:P43686-2 P17066:P48741 P02785:P02787 P40227:P40227-2:J3KR16 P62195:J3QJMT:J3QSE0:J3QRW1:J3KT Q9	26S protease regulatory subunit 6B	PSMC4	0.239815726	0.215152296	0.185328712	0.374695615	0.407262912	0.285617161	1.769471293	0.043301389
1:Z15:P11215-2 Q43242:H0VJG8:F5H8K4 Q9UNM6:13KNQ3:Q9UNM6- 2:A0A087WUL9:E9P138:H0YD73:E9PQG 3:E9PPD2:F8WB8 P10599:P10599-2 P43686:P43686-2 P17066:P48741 P02785:P02787 P40227:P40227-2:J3KR16 P62195:J3QJMT:J3QSE0:J3QRW1:J3KT Q9	Heat shock 70 kDa protein 6	HSPA6	0.02354706	0.031447754	0.047719256	0.055812556	0.067389213	0.070173697	1.748768923	0.016511504
1:Z15:P11215-2 Q43242:H0VJG8:F5H8K4 Q9UNM6:13KNQ3:Q9UNM6- 2:A0A087WUL9:E9P138:H0YD73:E9PQG 3:E9PPD2:F8WB8 P10599:P10599-2 P43686:P43686-2 P17066:P48741 P02785:P02787 P40227:P40227-2:J3KR16 P62195:J3QJMT:J3QSE0:J3QRW1:J3KT Q9	T-complex protein 1 subunit delta	CTC4	0.005575232	0.004673363	0.003238244	0.00849115	0.007180554	0.007294403	1.734917661	0.014895445
1:Z15:P11215-2 Q43242:H0VJG8:F5H8K4 Q9UNM6:13KNQ3:Q9UNM6- 2:A0A087WUL9:E9P138:H0YD73:E9PQG 3:E9PPD2:F8WB8 P10599:P10599-2 P43686:P43686-2 P17066:P48741 P02785:P02787 P40227:P40227-2:J3KR16 P62195:J3QJMT:J3QSE0:J3QRW1:J3KT Q9	T-complex protein 1 subunit zeta	CTC6A	0.010979883	0.00777022	0.005994958	0.015238795	0.013504136	0.01416762	1.724105636	0.017214999
1:Z15:P11215-2 Q43242:H0VJG8:F5H8K4 Q9UNM6:13KNQ3:Q9UNM6- 2:A0A087WUL9:E9P138:H0YD73:E9PQG 3:E9PPD2:F8WB8 P10599:P10599-2 P43686:P43686-2 P17066:P48741 P02785:P02787 P40227:P40227-2:J3KR16 P62195:J3QJMT:J3QSE0:J3QRW1:J3KT Q9	26S protease regulatory subunit 8	PSMC5	0.25575475	0.227850594	0.251653906	0.419041315	0.459439402	0.384446856	1.690446162	0.004264249
1:Z15:P11215-2 Q43242:H0VJG8:F5H8K4 Q9UNM6:13KNQ3:Q9UNM6- 2:A0A087WUL9:E9P138:H0YD73:E9PQG 3:E9PPD2:F8WB8 P10599:P10599-2 P43686:P43686-2 P17066:P48741 P02785:P02787 P40227:P40227-2:J3KR16 P62195:J3QJMT:J3QSE0:J3QRW1:J3KT Q9	26S proteasome non-ATPase regulatory subunit 11	PSMD11	0.176558215	0.169195837	0.192050797	0.324160822	0.306906059	0.273815082	1.68317239	0.001658485
1:Z15:P11215-2 Q43242:H0VJG8:F5H8K4 Q9UNM6:13KNQ3:Q9UNM6- 2:A0A087WUL9:E9P138:H0YD73:E9PQG 3:E9PPD2:F8WB8 P10599:P10599-2 P43686:P43686-2 P17066:P48741 P02785:P02787 P40227:P40227-2:J3KR16 P62195:J3QJMT:J3QSE0:J3QRW1:J3KT Q9	26S proteasome non-ATPase regulatory subunit 12	PSMD12	0.153654773	0.138221274	0.172209806	0.230342128	0.232389035	0.290505374	1.623054295	0.011927968
1:Z15:P11215-2 Q43242:H0VJG8:F5H8K4 Q9UNM6:13KNQ3:Q9UNM6- 2:A0A087WUL9:E9P138:H0YD73:E9PQG 3:E9PPD2:F8WB8 P10599:P10599-2 P43686:P43686-2 P17066:P48741 P02785:P02787 P40227:P40227-2:J3KR16 P62195:J3QJMT:J3QSE0:J3QRW1:J3KT Q9	Thioredoxin	TXN	0.010303226	0.007898252	0.010909952	0.018689351	0.015719683	0.017505678	1.789493409	0.004089853
1:Z15:P11215-2 Q43242:H0VJG8:F5H8K4 Q9UNM6:13KNQ3:Q9UNM6- 2:A0A087WUL9:E9P138:H0YD73:E9PQG 3:E9PPD2:F8WB8 P10599:P10599-2 P43686:P43686-2 P17066:P48741 P02785:P02787 P40227:P40227-2:J3KR16 P62195:J3QJMT:J3QSE0:J3QRW1:J3KT Q9	26S protease regulatory subunit 6B	PSMC4	0.239815726	0.215152296	0.185328712	0.374695615	0.407262912	0.285617161	1.769471293	0.043301389
1:Z15:P11215-2 Q43242:H0VJG8:F5H8K4 Q9UNM6:13KNQ3:Q9UNM6- 										